

RESEARCH PAPER

Polyols in grape berry: transport and metabolic adjustments as a physiological strategy for water-deficit stress tolerance in grapevine

Artur Conde^{1,2}, Ana Regalado³, Diana Rodrigues², J. Miguel Costa^{3,4}, Eduardo Blumwald⁵,
M. Manuela Chaves^{3,4} and Hernâni Gerós^{1,2,*}

¹ Centro de Investigação e de Tecnologias Agro-Ambientais e Biológicas (CITAB-UM), Portugal

² Grupo de Investigação em Biologia Vegetal Aplicada e Inovação Agroalimentar (AgroBioPlant), Departamento de Biologia, Universidade do Minho, 4710-057 Braga, Portugal

³ Instituto de Tecnologia Química e Biológica, Apartado 127, 2781-901 Oeiras, Portugal

⁴ Instituto Superior de Agronomia, Universidade Técnica de Lisboa, Tapada da Ajuda, 1349-017 Lisboa, Portugal

⁵ Department of Plant Sciences, UC Davis, One Shields Ave, Davis, CA 95616, USA

* To whom correspondence should be addressed. E-mail: geros@bio.uminho.pt

Received 28 June 2014; Revised 6 October 2014; Accepted 10 October 2014

Abstract

Polyols are important metabolites that often function as carbon and energy sources and/or osmoprotective solutes in some plants. In grapevine, and in the grape berry in particular, the molecular aspects of polyol transport and metabolism and their physiological relevance are virtually unknown to date. Here, the biochemical function of a grapevine fruit mesocarp polyol transporter (*VvPLT1*) was characterized after its heterologous expression in yeast. This H⁺-dependent plasma membrane carrier transports mannitol ($K_m=5.4$ mM) and sorbitol ($K_m=9.5$ mM) over a broad range of polyols and monosaccharides. Water-deficit stress triggered an increase in the expression of *VvPLT1* at the fully mature stage, allowing increased polyol uptake into pulp cells. Plant polyol dehydrogenases are oxidoreductases that reversibly oxidize polyols into monosaccharides. Mannitol catabolism in grape cells ($K_m=30.1$ mM mannitol) and mature berry mesocarps ($K_m=79$ mM) was, like sorbitol dehydrogenase activity, strongly inhibited (50–75%) by water-deficit stress. Simultaneously, fructose reduction into polyols via mannitol and sorbitol dehydrogenases was stimulated, contributing to their higher intracellular concentrations in water-deficit stress. Accordingly, the concentrations of mannitol, sorbitol, galactinol, *myo*-inositol, and dulcitol were significantly higher in berry mesocarps from water-deficit-stressed Tempranillo grapevines. Metabolomic profiling of the berry pulp by GC-TOF-MS also revealed many other changes in its composition induced by water deficit. The impact of polyols on grape berry composition and plant response to water deficit stress, via modifications in polyol transport and metabolism, was analysed by integrating metabolomics with transcriptional analysis and biochemical approaches.

Key words: Grape berry metabolome, osmoprotection, polyol metabolism, polyol/sugar ratio, polyol transport, *VvPLT1*, water-deficit stress.

Introduction

Vitis vinifera L. is a plant species with relatively high water-deficit stress tolerance (Grimplet *et al.*, 2007). However, the combined effect of drought, high air temperature, and high evaporative demand during summer in areas such as the

Mediterranean basin limits grapevine yield and berry development (Chaves *et al.*, 2007; Costa *et al.*, 2007). Dramatic reductions in plant carbon assimilation may occur because of a severe decline in photosynthesis under high leaf temperatures

combined with water deficits, and as a consequence of a partial loss of canopy leaf area (Flexas *et al.*, 1998, 2002; Maroco *et al.*, 2002; Souza *et al.*, 2005). The use of irrigation in these harsh environments arises as a solution to avoid excessive canopy temperature, maintain quality in fruit and wine production, and, in more extreme cases, guarantee plant survival. Nevertheless, grapevine irrigation is a subject under considerable debate, as small water supplements may increase yield and maintain and even improve berry quality (Matthews and Anderson, 1989). However, it can also promote excessive vegetative growth with a negative impact on berry colour, aroma, and sugar content, and in increasing titratable acidity, therefore decreasing wine quality and flavours (reviewed by Chaves *et al.*, 2010). The large canopy leaf area resulting from prolonged irrigation also tends to increase the incidence of fungal diseases (Dry and Loveys, 1998).

Understanding the physiological and molecular mechanisms of plant responses to moderate water deficits is critical to modulate the appropriate balance between vegetative and reproductive development, to improve crop water use (Blum, 2009), and to control fruit quality under deficit irrigation (Chaves *et al.*, 2007). Regulated deficit irrigation (RDI) has been used to improve berry and wine quality (Roby *et al.*, 2004; Chapman *et al.*, 2005), and application of water deficit early in the season before véraison promoted increased concentrations of anthocyanins and phenolics (Matthews and Anderson, 1988; Matthews *et al.*, 1990; Deluc *et al.*, 2009). Moreover, the timing and intensity of water deficits influence the extent of changes in berry metabolism and in wine colour, aroma, and flavour by modifying berry size and/or the synthesis of berry compounds, with a positive contribution to the fruit and wine organoleptic properties. Indeed, a water-deficit treatment typically increases the skin to pulp ratio in the berries, when compared with well-watered grapevines (Ojeda *et al.*, 2002; Roby *et al.*, 2004), increasing the amount of skin tannins and anthocyanins. Colour differences may result from increased anthocyanin synthesis caused by water deficit applied either early or late in the season (Matthews and Anderson, 1988; Castellarin *et al.*, 2007). Water deficit triggers an increase in the concentration of the abiotic stress signalling molecule abscisic acid (ABA) in the xylem sap and leaves of grapevine, through a mechanism that may activate a series of signalling pathways involved in water-deficit stress tolerance.

In general, to overcome the effects of abiotic stresses, plants have developed complex and dynamic systems involving a wide range of biochemical and physiological processes (Vincent *et al.*, 2007; Ahuja *et al.*, 2010; Cramer *et al.*, 2011; Saidi *et al.*, 2011; Walbot *et al.*, 2011). Among these, the accumulation of compatible solutes consisting of non-toxic organic molecules, such as polyols (or sugar alcohols), protects the cells against deleterious osmotic and metabolic imbalances caused by stress (Conde *et al.*, 2011a; Pillet *et al.*, 2012). Polyols are the reduced form of aldoses and ketoses, and are present in all living forms (Noiraud *et al.*, 2001a). In some plants, these polyols are, together with sucrose (as in celery) or raffinose saccharides (as in olive), direct products of photosynthesis and serve similar functions such as the

translocation of carbon skeletons and energy between source and sink organs. Mannitol is the most widespread polyol in nature, and has been observed in >100 vascular plant species of several families including the Apiaceae (celery, carrot, and parsley), Rubiaceae (coffee), and Oleaceae (olive and privet) (Lewis, 1984). In olive and celery, mannitol synthesis takes place in mature leaves from mannose-6-phosphate by the action of an NADPH-dependent mannose-6-phosphate reductase (M6PR) that synthesizes mannitol-1-phosphate followed by dephosphorylation by mannitol-1-phosphate phosphatase. It is then translocated through the phloem to heterotrophic sink tissues where it can be either stored or oxidized to mannose via the action of a 1-oxireductase, NAD⁺-dependent mannitol dehydrogenase (MTD), and used as a carbon and energy source (reviewed by Stoop *et al.*, 1996; Noiraud *et al.*, 2001b; Conde *et al.*, 2008). Mannitol accumulation is a crucial mechanism for salt/osmotic stress tolerance in *Olea europaea* (Conde *et al.*, 2011b), but also for coping with heat stress-induced oxidative damage and excessive solar irradiance (Melgar *et al.*, 2009; Remorini *et al.*, 2009; Cimato *et al.*, 2010). The introduction and overexpression of an *Escherichia coli* mannitol-1-phosphate dehydrogenase (*mtlD*) gene in plants such as tobacco, *Arabidopsis*, wheat, and *Populus tomentosa* resulted in the accumulation of mannitol and consequent increased tolerance to water deficit or salinity (Tarczynski *et al.*, 1993; Thomas *et al.*, 1995; Karakas *et al.*, 1997; Abebe *et al.*, 2003; Hu *et al.*, 2005). According to KEGG (Kyoto Encyclopedia of Genes and Genomes; Kanehisa and Goto, 2000), and differing from olive and celery, the main product of mannitol oxidation in grapevine is fructose, in an NAD⁺-dependent reaction catalysed by the oxireductase mannitol dehydrogenases (EC 1.1.1.67).

Another polyol present widely in higher plants is sorbitol, a major translocated photoassimilate, in the phloem of woody Rosaceae, including all members of the economically important genera *Pyrus* (pear), *Malus* (apple), and *Prunus* (stone fruits such as peach, cherry, plum, and apricot; Zimmermann and Ziegler, 1975; Bieleski, 1982; Moing *et al.*, 1997). In higher plants, sorbitol is synthesized in mature leaves from glucose-6-phosphate by the consecutive activities of an aldose-6-P-reductase (Negm and Loescher, 1981) and a specific phosphatase. In general, sinks have little or no capacity to synthesize polyols such as mannitol or sorbitol (Loescher and Everard, 1996; Nawodnik and Lohaus, 2008). In the sucrose- and sorbitol-translocating species *Plantago major*, salt stress promotes a higher sorbitol to sucrose ratio in the phloem sap (Pommerrenig *et al.*, 2007), with sorbitol concentrations rising up to 10 mg g⁻¹ fresh weight (FW). Sorbitol synthesis/accumulation also contributed to increased salt/water-deficit tolerance in peach, persimmon tree, and even tomato (Escobar-Gutiérrez *et al.*, 1998; Gao *et al.*, 2001; Tari *et al.*, 2010; reviewed by Krasensky and Jonak, 2012). In grapevine, according to KEGG (Kanehisa and Goto, 2000), sorbitol is primarily and reversibly oxidized to sorbose or fructose in an NAD⁺-dependent reaction catalysed by a sorbitol dehydrogenase (EC 1.1.1.15).

Although transcripts putatively encoding polyol dehydrogenases and transporters had been previously detected in

general transcriptomic profiling (Deluc *et al.*, 2007; Afoufa-Bastien *et al.*, 2010), little is known about polyol transport steps and metabolism in grapevine and their physiological relevance in the plant, particularly in the grape berry. In addition, the impact and protective role of polyols in water deficit and salinity tolerance in some plants has been recognized, such as in *O. europaea*, celery, and common plaintain (Tarczynski *et al.*, 1993; Williamson *et al.*, 1995; Stoop *et al.*, 1996; Conde *et al.*, 2007a, 2011b; Pommerrenig *et al.*, 2007), but no physiological roles had been attributed to date in grapevine.

In the present study, a multidisciplinary approach was adopted, combining an array of molecular biology, classic biochemical, recent metabolomic, and transcriptional analysis approaches as tools to reveal a function for polyols in grapevine [Tempranillo cv. (syn Aragonez)] water-deficit stress tolerance, and to uncover the influence of polyol transport and modifications of its metabolism in osmoprotection, at both the cellular and whole-plant physiological/eco-physiological levels, with a particular emphasis on the grape berry.

Materials and methods

Grapevine field conditions and water-deficit treatments

Field-grown grapevines (*Vitis vinifera* L.) of ‘Tempranillo’ (syn. Aragonez) variety from a commercial vineyard (Monte Seis Reis) located in Estremoz (38°48′N, 7°29′W), Alentejo (South Portugal) were used in the present study. The climate is typically Mediterranean, with hot, dry summers and mild air temperatures, with precipitation concentrated during autumn and winter.

Three different irrigation treatments were applied to the Tempranillo vines: full irrigation [FI; 100% evapotranspiration (ET_c)]; non-irrigation (NI; rain fed only), and RDI (50% ET_c). Watering was applied according to crop ET_c and soil water content. ET_c was estimated from the ET_o , using the crop coefficients (K_c) proposed by the FAO (1998). Drip irrigation lines were positioned along plant rows and consisted of pressure-compensating 2.5 L h⁻¹ emitters with 1 m of spacing, one per vine, positioned between two adjacent grapevines. Irrigation treatments started after flowering, thus at the beginning of berry development (early June), and lasted until harvest (early September). The average maximum temperature and average relative humidity during this period were 28.2 °C and 53%, respectively.

To obtain physiologically representative samples, grape berry clusters from 4–6 plants subjected to the different irrigation regimes, located in three different rows, were collected, and grapes from three different berry clusters per plant were harvested and immediately frozen in liquid nitrogen. FI, NI, and RDI berries were collected at the green stage [44 days after flowering (DAF)], véraison (62 DAF), mature stage (77 DAF), and fully mature stage (97 DAF) of berry development, according to the BBCH phenological scale of grapevine (Lorenz *et al.*, 1994). The average maximum temperatures during the 48 h period before sample collection were 29.0 °C at the green stage, 31.6 °C at véraison, 33.3 °C at the mature stage, and 29.1 °C at the fully mature stage, whereas the average relative humidity during the same periods was 45, 44, 45, and 46%, respectively.

The exocarps and seeds were carefully removed in continuous liquid nitrogen refrigeration to obtain the berry mesocarps, which were subsequently stored at –80 °C.

In parallel, 5- to 6-year-old potted plants of *V. vinifera* cv. Tempranillo (syn. Aragonez), grafted on the 1103-P rootstock, were grown in a greenhouse at the ITQB, Oeiras (38°41′N; 9°19′W) in 40 litre pots containing a medium texture soil with a pH 6.2, 4.3% organic matter, and an electrical conductivity (EC) of 0.38 mS cm⁻¹, with semi-controlled ventilation, and air temperature and relative

humidity monitoring with a Lufft 8147 Quartz Thermohygrograph (Lufft, Germany). FI (control), with watering of the plants every 2 d, and NI regimes were applied to the potted grapevines for a period of 4 weeks. The mean air temperature and relative humidity during treatment were 22.0 °C and 46%, respectively. Plants were grown under natural light and photoperiod (16 h of daily light) with an average photon flux density of ~500 μmol m⁻² s⁻¹. Plant water status was assessed during the experiment by measuring leaf water potential at pre-dawn (Ψ_{pd}) with a Scholander pressure chamber. Leaves from 6–8 independent plants for each irrigation regime were harvested at the end of the treatment, when the plant water potential of stressed plants was $-1.3 < \Psi_{pd} < -0.9$ MPa. Samples were immediately frozen in liquid nitrogen and stored at –80 °C.

Grapevine cell suspensions, growth conditions, and osmotic/salt stress treatments

Cell suspensions of *V. vinifera* L. [Cabernet Sauvignon Berry (CSB)] were freshly established from somatic callus that had been previously initiated from Cabernet Sauvignon berry pulp according to Calderón *et al.* (1994). They were maintained in 250 ml flasks at 25 °C in the dark on a rotator shaker at 100 rpm, on modified Murashige and Skoog (MS) medium (Murashige and Skoog, 1962; Decendit *et al.*, 1996), supplemented with either one of the following carbon sources, depending on the purpose: 1% (w/v) glucose, 0.5% (w/v) mannitol+0.5% (w/v) glucose, or 0.5% (w/v) sorbitol+0.5% (w/v) glucose. The suspension-cultured cells were subcultured weekly by transferring 10 ml aliquots into 40 ml of fresh medium. Cell growth was assayed as previously described (Conde *et al.*, 2006). Salt (and, as a consequence, osmotic) stress was induced by addition of a final concentration of 100 mM NaCl ($\Psi = -0.4$ MPa). To simulate osmotic stress-only conditions, polyethylene glycol (PEG 8000) was added at a final concentration of 15% (w/v) to provide the –0.4 MPa of water potential reached with 100 mM NaCl, a value regarded as moderate osmotic stress in plant tissues. Depending on the study, the stress treatments were carried out either for a 24 h period at the mid-exponential growth phase of the cells, or during the whole cellular growth phase until the end of the exponential and subsequent stationary phase.

RNA extraction, VvPLT1 and VvMTD1 molecular cloning, and construction of VvPLT1–GFP fusion protein

A total of 200 mg of grape berry mesocarp tissue previously ground in liquid nitrogen was used for total RNA extraction (Reid *et al.*, 2006). The obtained RNAs were then purified on RNeasy Mini Spin columns (Qiagen). After treatment with DNase I (Qiagen), cDNA was synthesised from 1 μg of total RNA using a Qiagen Omniscript Reverse Transcription Kit.

Gateway® technology was used for cloning *VvPLT1* and *VvMTD1*, and for VvPLT1–green fluorescent protein (GFP) construction. Gene-specific primers with adjacent oligonucleotide sequences (*attB* primers) (Supplementary Table S4 available at JXB online) for site-specific recombination with the plasmid pDONR221 were used for PCR amplification of *VvPLT1* and *VvMTD1*. The reverse primer *attB-VvPLT1rev-egfp* was designed without the codon stop of the *VvPLT1* open reading frame (ORF) ultimately to allow a C-terminal fusion with *egfp*. BP clonase (Invitrogen) was used in the BP recombination reaction with pDONR221 to obtain entry clones (*pDONR221-VvPLT1* and *pDONR221-VvMTD1*), and gene sequencing was performed for confirmation on positive clones. After *VvPLT1* and *VvMTD1* sequencing in *pDONR221*, LR clonase (Invitrogen) was used in the LR recombination reaction of *pDONR221-VvPLT1* with *pYES-DEST52* for heterologous expression in yeast and functional studies, or with *pH7FWG2.0*, containing the *egfp* gene, for the construction of VvPLT1–GFP and subcellular localization in tobacco. The final constructs *pYES-DEST52-VvPLT1* and *VvPLT1-egfp* were also confirmed by sequencing.

Heterologous expression of VvPLT1 in Saccharomyces cerevisiae

The yeast strain MaDH4 (*ura3, trp1, LEU2, gap1-1, put4-1, uga4-1*) (Noiraud *et al.*, 2001a) was used for functional characterization of *VvPLT1*. The yeast transformation with *pYES-DEST52-VvPLT1* was performed following the Gietz and Woods (2002) LiAc/SS carrier DNA/PEG method. For the control, MaDH4 yeast cells were transformed with *pYES-DEST52* plasmid without *VvPLT1*. The yeast transformants were selected by growth in 2% (w/v) glucose Yeast Nitrogen Base (YNB) medium without uracil.

Polyol transport studies in S. cerevisiae

Yeast MaDH4 cells transformed with *pYES-DEST52-VvPLT1* (or empty *pYES-DEST52*, for control cells) were grown in YNB 2% (w/v) galactose medium, at 30 °C, on a rotator shaker at 200 rpm, to an OD₆₀₀ of ~0.8, to induce the highest possible expression of *VvPLT1*, which is under the regulation of the galactose-inducible promoter *GAL1* of the *pYES-DEST52* plasmid. Yeast cells were then harvested by centrifugation, washed twice with ice-cold sterile distilled water, and suspended in 25 mM MES buffer (pH 4.5) at a final concentration of ~30 mg dry weight (DW) ml⁻¹.

To characterize *VvPLT1* functionally and estimate initial uptake rates of radiolabelled mannitol, 20 µl of cell suspension were mixed with 25 µl of 25 mM MES buffer at pH 4.5 in 10 ml conical tubes. After 2 min of incubation at 28 °C in a water bath, the reaction was started by the addition of 5 µl of an aqueous solution of radiolabelled mannitol with a specific activity of either 750 (20 mM), 1000 (10 mM), 2000 (5 mM), or 8000 dpm nmol⁻¹ (0.2–2 mM) (D-[¹⁴C]mannitol) at the desired final concentration. The same reaction conditions were used to estimate initial uptake rates of radiolabelled sorbitol, but using 5 µl of aqueous solutions with specific activities and final concentrations as follows: 1000 (10 mM), 2000 (5 mM), or 8000 dpm nmol⁻¹ (0.1–2 mM) (D-[¹⁴C]sorbitol) at the desired final concentration. Potential competitive inhibitors or CCCP (carbonyl cyanide *m*-chlorophenylhydrazone) were added to the reaction mixture immediately before the addition of the radiolabelled polyol. The reaction was stopped by dilution with 10 ml of ice-cold water, and the mixtures were immediately filtered through GF/C filters (Whatman, Clifton, NJ, USA). The filters were washed with 10 ml of ice-cold water and transferred to vials containing scintillation fluid, and the radioactivity was measured in a scintillation counter. D-[¹⁴C]Mannitol (58.8 mCi mmol⁻¹) was obtained from Perkin-Elmer (Waltham, MA, USA) and D-[¹⁴C]sorbitol (300 mCi mmol⁻¹) was obtained from American Radiolabelled Chemicals (St. Louis, MO, USA).

Transport studies with radiolabelled mannitol in CSB cells

CSB cells were cultivated in the dark at 100 rpm and 25 °C with 0.5% (w/v) mannitol+0.5% (w/v) glucose until mid-exponential growth phase, subjected to 100 mM NaCl or 15% PEG for 24 h, and then collected. Harvested control and treated cells were centrifuged, washed twice with ice-cold culture medium without sugars at pH 4.5, and re-suspended in the same medium at a final concentration of 5 mg DW ml⁻¹. To estimate the initial uptake rates of D-[¹⁴C]mannitol, 1 ml of each cell suspension was added to 10 ml flasks, with shaking at 100 rpm. After 2 min of incubation at 25 °C, the reaction was started by the addition of 40 µl of an aqueous solution of radiolabelled mannitol at the desired specific activity and concentration. The specific activities were defined according to the final concentration of the polyol in the reaction mixture, as follows: 1000 dpm nmol⁻¹ (0.1–2 mM), 500 dpm nmol⁻¹ (5–20 mM). Washing and radioactivity measurements were performed as described above.

Quantification of the intracellular concentration of mannitol in CSB cells

To determine the effect of 100 mM NaCl and 15% (w/v) PEG on the intracellular concentration of mannitol in CSB cells cultivated

in the dark at 100 rpm and 25 °C in the presence of 0.5% (w/v) mannitol+0.5% (w/v) glucose, stressed and control CSB cells were grown until mid-exponential phase, harvested, and washed twice in ice-cold culture medium without sugar and polyol, and then filtered and immediately frozen in liquid nitrogen. The extraction of sugars and sugar alcohols from the grape cells was performed as described by Eyéghé-Bickong *et al.* (2012) using cells instead of grape berry tissue. The extracted carbohydrates were filtered and quantified by HPLC-RI using a Rezex RCM–Monosaccharide Ca²⁺ (8%) column (Phenomenex) at a flow rate of 0.5 ml min⁻¹ at 40 °C using ultrapure water as the mobile phase. The injection volume was 20 µl, and 1% (w/v) mannitol, 1% (w/v) glucose, and 1% (w/v) fructose were used as standard solutions, while 1% (w/v) arabinol was used as internal standard.

Mannitol dehydrogenase and sorbitol dehydrogenase activity measurements in grape berries and CSB cells

Protein extraction and mannitol dehydrogenase (VvMTD) or sorbitol dehydrogenase (VvSDH) activity determination were carried out following Stoop and Pharr (1993). Grape berry mesocarps were ground using a chilled mortar and pestle in an ~1:2 (v/v) powder:buffer ratio, whereas CSB suspension-cultured cells were treated and harvested as described above and also ground using a chilled mortar and pestle in a 1:1 (v/v) powder:buffer ratio. The protein extraction buffer contained 50 mM MOPS (pH 7.5), 5 mM MgCl₂, 1 mM EDTA, 1 mM phenylmethylsulphonyl fluoride (PMSF), 5 mM dithiothreitol (DTT), 1% (v/v) Triton X-100, and 1% (w/v) polyvinylpyrrolidone (PVPP). The homogenates were thoroughly mixed and centrifuged at 18 000 g for 20 min, and the supernatants were maintained on ice and used in the enzymatic assays. VvMTD and VvSDH activity assays were performed at 37 °C, in a total reaction volume of 1 ml. The reaction mixtures contained protein extract, 300 mM BIS-TRIS propane (pH 9.0), 1 mM NAD⁺, and D-mannitol or D-sorbitol at the desired final concentration, for VvMTD or VvSDH activity, respectively. The reduction of NAD⁺ was evaluated spectrophotometrically at 340 nm. All polyol oxidation reactions were initiated by the addition of the polyol. To evaluate the effects of water-deficit stress (NI) on grape berry VvMTD and VvSDH activities, and the effect of salt and osmotic stresses in CSB cells, 200 mM of the desired polyol was used to ensure the V_{max} of mannitol or sorbitol oxidation. The MTD activity measurements in the direction of fructose reduction were performed exactly like the mannitol oxidation assays, but using 200 mM fructose to start the reaction and 1 mM NADH as co-factor. Total protein concentrations of the extracts were determined by the method of Bradford (1976) using bovine serum albumin as a standard.

Gene expression analysis by real-time qPCR

All gene expression analysis of *VvPLT1*, *VvMTD1*, and *VvSDH1* on grape berry mesocarps at different developmental stages in vines subjected to different irrigation regimes or in CSB cells subjected to the previously described conditions were performed by real-time quantitative PCR (qPCR). A QuantiTect SYBR Green PCR Kit (Qiagen) was used for qPCR analysis, using 1 µl of cDNA (diluted 1:10 in ultra-pure distilled water) in a final reaction volume of 20 µl per well. For reference genes, *VvACT1* (actin) and *VvGAPDH* (glyceraldehyde-3-phosphate dehydrogenase), two genes proven to be very stable and ideal for qPCR normalization purposes in grapevine (Reid *et al.*, 2006), were chosen. Gene-specific primer pairs used for each target or reference gene and amplicon length are listed in Supplementary Table S4 at JXB online. Melting curve analysis was performed for specific gene amplification confirmation. The efficiencies of the PCR for each gene were assessed using serial dilutions of template cDNA and were taken into account for gene expression values. The expression values of *VvPLT1*, *VvMTD1*, and *VvSDH1* are normalized by the average of the expression of the reference genes as described by Pfaffl (2001). For all experimental conditions

tested, three independent experiments, one for each biological replicate, with duplicates were performed.

Metabolomic analysis of grape berries and leaves by GC-TOF-MS

Metabolite extraction from the lyophilized samples and analysis by gas chromatography–time of flight-mass spectrometry (GC-TOF-MS) were carried out in the UC Davis Genome Center Metabolomics Laboratory as described by Fiehn *et al.*, (2008). After metabolite extraction and derivatization, samples were injected in split-less mode with a cold injection system (Gerstel, Germany) and analysed by GC (Agilent 6890, San Jose, CA, USA) using an Rtx 5Sil MS column (30 m×0.25 mm, 0.25 µm film thickness) and an integrated guard column (Restek, Bellefonte, PA, USA). The gas chromatograph was connected to a Leco Pegasus IV TOFMS spectrometer controlled with Leco ChromaTOF software v.2.32 (Leco, St. Joseph, USA). Peak detection and mass spectra deconvolution were performed with Leco Chroma-TOF software v.2.25. GC-MS chromatograms were processed following Fiehn *et al.* (2008). Further analysis after deconvolution was made using the semi-automated workflow of the UC Davis Genome Center Metabolomics Laboratory (Fiehn *et al.*, 2005). Metabolite data were normalized using the dry (lyophilized) weight (DW) of the samples. Several polyols, among a wide variety of other metabolites, were detected by the GC-TOF-MS analysis, but only mannitol, sorbitol, galactinol, *myo*-inositol, glycerol, and dulcitol were quantified. For the rest of the metabolites, data transformation (\log_2) and normalization were performed using GeneMaths XT software, in which the offset was determined by the average of relative abundance values and the scaling was defined according to the standard deviation. Heat maps were performed to discriminate grape berry mesocarp and leaf metabolite profiles and to compare the changes in metabolite concentration throughout fruit development induced by water-deficit stress treatment (NI). For all experimental conditions, three independent runs were performed in all metabolomic analysis.

Subcellular localization of VvPLT1–GFP

Transient expression of the construct *P35:VvPLT1-GFP* in leaf abaxial epidermal cells of tobacco (*Nicotiana tabacum*) was performed following the agroinfiltration protocol described by Voynet *et al.* (2003) using the *Agrobacterium* strain GV3101 transformed by electroporation with the corresponding constructs and plasmids.

Agro-infiltrated tissue samples were examined 4 d after transformation using an Olympus FluoView FV1000 confocal microscope (Olympus, Inc., Cener Valley, PA, USA). GFP fluorescence was excited using a 488 nm laser, and yellow fluorescent protein (YFP) fluorescence at 514 nm, with GFP and YFP fluorescence detection being collected between 500 nm and 560 nm, and between 535 nm and 590 nm, respectively. Captured images were further processed using Adobe Photoshop software (Adobe Systems, Inc., San Jose, CA, USA).

Accession numbers

Sequence data from VvPLT1 and VvMTD1 can be found in the GenBank/EMBL data libraries under the accession numbers KF319032 and KF319033, respectively. Other sequence data used in this article can be found in the same data libraries, as follows: VvPLT1 orthologues: NP_001147446.1 (ZmSOT1), BAC83310.1 (OsSOT1), XP_003562818.1 (BdPLT1), DAA45950.1 (ZmPLT1), CAJ29288.1 (LjPLT1), Q9ZNS0 (AtPLT3), Q0WUU6 (AtPLT4), Q8GXR2 (AtPLT6), XP_003541068.1 (GmPLT1), NP_001236592.1 (GmSOT1), ACD68477.1 (AhMaT1), XP_003603886.1 (MtMaT1), ACB86853.1 (CsMaT1), XP_002885281.1 (AtPLT5), NP_179209.1 (AtPLT1), NP_179210.1 (AtPLT2), AAB68029.1 (BvSTP1), XP_004230909.1 (SIPLT1), XP_002519083.1 (RcSTP1), CAP58707.1 (HbPLT2), CAP58706.1 (HbPLT1), XP_002313809.1 (PtPLT1), XP_004148857.1

(CsPLT1), AAM44082.1 (PcSOT1), BAD42345.1 (MdSOT1), XP_004299107.1 (FvPLT1), AAO39267.1 (PcSOT2), EMJ00992.1 (PpPLT1), ACB56939.1 (AaMaT1), AFI61955.1 (CasPLT1), AAL85876.2 (AgMaT2), AAY88181.2 (OeMaT1), AAG43998.1 (AgMaT1), CA D58710.1 (PmPLT1), A9RMV5 (PhyPLT1). Other putative VvPLTs: A5BUJ3 (VvPLT2), E3VWW0 (VvPLT4), E3VWW1 (VvPLT3), E3VWW3 (VvPLT5). VvMTD1 orthologues: NP_001147757.1 (ZmMTD1), A2YT96 (OsMTD1), A9T4F7 (PhyMTD1), O82515.1 (MsMTD1), XP_002313297.1 (PtCAD1), EMJ06615.1 (PpMTD1), Q9ZRF1.1 (FaMTD1), XP_004288496.1 (FvMTD1), XP_002534367.1 (RcADH1), NP_001031805.1 (AtMTD1 (ELI3)), XP_003612973.1 (MtCAD1), P93257.1 (McMTD1), XP_003517258.1 (GmMTD1), XP_004250191.1 (SIMTD1), XP_004143438.1 (CsMTD1), ABR31791 (OeMTD1), 2117420A (AgMTD1), P42754.1 (PcMTD1). AtPIP1;4, Q39196; VvSDH1, XP_002269895; VvA6PR, XP_002269232.1.

Results

Metabolomic analysis of grape berries and leaves in response to water-deficit stress

The metabolome analysis by GC-TOF-MS detected a total of 458 metabolites in grape berries and leaves from Tempranillo vines, 154 of which were unequivocally identified, ranging from sugars, polyols, organic acids, amino acids, to some secondary metabolites (Supplementary Figs S1, S2 at JXB online). The changes in the profile of a large number of metabolites in developing grape berries upon water-deficit stress clearly demonstrated the strong influence of water deficit in the metabolome of this fruit that would eventually modify the wine characteristics. Six (mannitol, sorbitol, galactinol, *myo*-inositol, glycerol, and dulcitol) of the 10 identified polyols were further quantified.

Mannitol and sorbitol were significantly accumulated in the pulp of grape berries in response to water deficit (Fig. 1). In NI and fully mature [15 weeks after flowering (WAF)] grape berries mannitol reached a concentration of 2 mg g⁻¹ DW, 2.5-fold higher than in FI berries. This considerable difference between FI and NI berries was maintained in all maturation stages. Moreover, RDI also induced an accumulation of mannitol in the pulp of grape berries in all ripening stages, but less pronounced than in the most significant water deficit condition (NI), as can be observed particularly in the green stage (5 WAF). In control (FI) conditions, the concentration of mannitol hardly changed from one developmental stage to another.

Sorbitol accumulation in the grape berry pulp of water-deficit-stressed grapevines was even more significant, with its concentration being 3- to 4- fold higher in NI than in FI berries in the later ripening stages (Fig. 1). In NI fully matured berries, the concentration of sorbitol was ~2.3 mg g⁻¹ DW, but the highest detected sorbitol concentration was in the mature berry stage (77 DAF) of vines subjected to RDI (2.9 mg g⁻¹ DW). Sorbitol concentration increased smoothly throughout grape berry development, a pattern more accentuated under RDI until the mature stage (77 DAF), followed by a decrease in the fully mature stage. In contrast, in FI vines, sorbitol concentration was relatively steady during berry ripening.

Galactinol also accumulated in the pulp of grape berry under water deficit (Fig. 2A), to a lower extent than mannitol

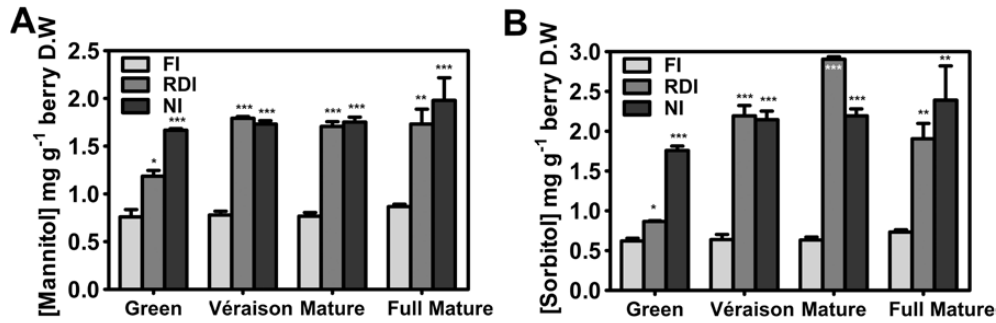


Fig. 1. Effect of water-deficit stress on the accumulation of mannitol and sorbitol in grape berries. Concentration of mannitol (A) and sorbitol (B) in grape berry mesocarps at different developmental stages in vines subjected to different irrigation regimes (FI, full irrigation; RDI, regulated deficit irrigation; NI, non-irrigation). Metabolomic analysis was performed by GC-TOF-MS. Values are the mean \pm SEM of three experiments. Asterisks indicate statistical significance (Student's *t*-test; * P <0.05; ** P <0.01; *** P <0.001).

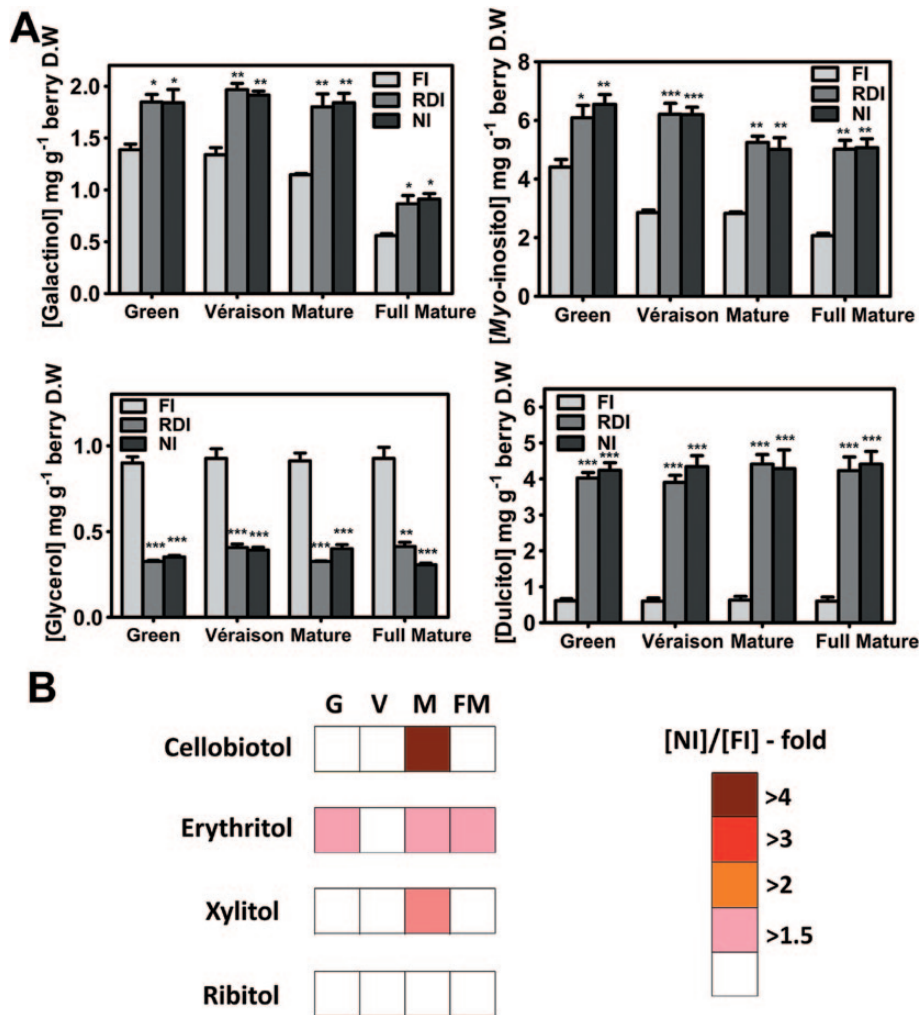


Fig. 2. Effect of water-deficit stress on the accumulation of galactinol, *myo*-inositol, glycerol, dulcitol, cellobiotol, erythritol, xylitol, and ribitol in grape berries. (A) Concentration of galactinol, *myo*-inositol, glycerol, and dulcitol, in grape berry mesocarps at different developmental stages in vines subjected to different irrigation regimes (FI, full irrigation; RDI, regulated deficit irrigation; NI, non-irrigation). Asterisks indicate statistical significance (Student's *t*-test; * P <0.05; ** P <0.01; *** P <0.001). (B) Relative amounts of cellobiotol, erythritol, xylitol, and ribitol in mesocarps from NI berries relative to FI berries (fold variation). Metabolomic analysis was performed by GC-TOF-MS. All values are the mean \pm SEM of three experiments.

or sorbitol. The concentration of galactinol was higher from the green to the mature stages, and it was ~50% higher (1.8 mg g⁻¹ DW) in NI and RDI than in FI berries. However, the galactinol concentration sharply decreased in fully mature grape berries in all irrigation treatments. *Myo*-inositol and

dulcitol were also present in higher concentrations in berries of grapevines subjected to water-deficit stress, but displayed different patterns of accumulation (Fig. 2A). The concentration of *myo*-inositol steadily decreased in control FI berries during ripening. In NI berries, a peak of 6.5 mg g⁻¹ DW of

myo-inositol was detected in the green stage, and the decrease during maturation was more subtle, with the contents of the fully mature berries being ~2-fold higher than in FI. A 5- to 6-fold accumulation of dulcitol was observed in response to water-deficit stress. Interestingly, glycerol followed a different pattern from that of all other quantified polyols in the berry, because its concentration was 2.5- to 3- fold lower in grape berries of water-deficit-stressed grapevines (Fig. 2A). For each irrigation treatment, glycerol concentrations were very similar in all ripening stages, with ~0.9 mg g⁻¹ DW in FI berries. Even polyols considered less important, or with a lesser known physiological role, such as cellobiotol, erythritol, and xylitol, increased their concentration in at least 50% at some point during berry ripening in NI (Fig. 2B). Among these polyols, the 4.4-fold accumulation of cellobiotol at the mature stage of NI berries, as compared with the control (FI), comprised the most significant polyol accumulation response to water-deficit stress. In NI, erythritol concentration was 52% higher at both the green and fully mature stages, and 82% higher in mature berries, whereas xylitol increased to almost 70% at this stage. On the other hand, ribitol berry amounts were not altered by water deficit.

Based on this strong polyol accumulation in grape berries as a response to water-deficit stress, an additional independent metabolomic analysis in mature leaves was performed to evaluate possible water deficit-induced changes in polyol concentrations and in its putative biosynthesis rate in mesophyll cells. Mannitol and galactinol concentrations were slightly higher under water deficit than in controls, whereas sorbitol, *myo*-inositol, glycerol, and dulcitol concentrations remained statistically the same (Fig. 3A). Overall, the most abundant of the quantified polyols in mature leaves was *myo*-inositol, with almost 12 mg g⁻¹ DW under NI, with mannitol and sorbitol reaching ~0.6 mg g⁻¹ DW and 0.4 mg g⁻¹ DW, respectively. Water deficit affected other polyols in different ways, from a strong increase in erythritol content (3.2-fold), to a 61% decrease in cellobiotol, or no change at all for xylitol and ribitol amounts in mature leaves (Fig. 3B).

In contrast to the polyol accumulation in the grape berry promoted by water-deficit stress, the concentrations of fructose and sucrose in mature grapes were 25% lower in NI (Fig. 4) and were inferior in all maturation stages, with the exception of sucrose quantities at véraison. Glucose, however, remained unaltered by water deficit in the final ripening stage. In leaves, only the sucrose concentration was lower (50%) in water-deficit conditions (Supplementary Fig. S3 at JXB online). In contrast, glucose and fructose concentrations increased upon water deficit.

Cloning and molecular characterization of the polyol transporter VvPLT1 and the mannitol dehydrogenase VvMTD1

A gene encoding a polyol transporter in grapevine, *VvPLT1* (*Vitis vinifera* polyol transporter 1), was cloned from the pulp tissues of fully mature berries from cv. Tempranillo. The amino acid sequence of VvPLT1 was analysed *in silico* and compared with other well characterized polyol transporters from several

plants, inducing more specific mannitol (AgMaT1, OeMaT1) or sorbitol transporters (PcSOT1), and less specific polyol transporters such as PmPLT1 and AtPLT5 (Supplementary Fig. S4 at JXB online). This carrier of polyols is a plasma membrane protein (Fig. 5) with 528 amino acid residues, sharing remarkable sequence identity with other plant polyol transporters, such as the mannitol transporter of *O. europaea* (OeMaT1; Conde *et al.*, 2007a). VvPLT1 belongs to the major facilitator superfamily (MFS) of membrane transport proteins, with 12 predicted transmembrane domains, and is part of the sugar transporter subfamily, as suggested by the two typical conserved GRR sequences, among other conserved sequences (Supplementary Fig. S4). The full-length VvPLT1 cDNA was fused at its C-terminus to GFP and transiently expressed under the control of the *Cauliflower mosaic virus* 35S promoter to confirm its plasma membrane location. The GFP fluorescence was clearly seen in the periphery of tobacco cells, confirming that VvPLT1-GFP localized at the plasma membrane (Fig. 5).

Based on *in silico* analysis, the polyol transporter VvPLT1 was shown to be part of a clade of five putative polyol transporters. VvPLT1 was the grapevine polyol transporter that shared by far the highest sequence identity with functional plasma membrane polyol transporters from other plants already described, including the mannitol transporters AgMaT1 and AgMaT2 from celery and OeMaT1 from olive, the polyol transporters AtPLT5 from *Arabidopsis* and PmPLT1 and PmPLT2 from *Plantago major*, and the sorbitol transporters PcSOT1 from *Prunus cerasus* and several sorbitol transporters from apple, with ~72–81% amino acid identity (Noiraud *et al.*, 2001a; Gao *et al.*, 2003; Ramsperger-Gleixner *et al.*, 2004; Watari *et al.*, 2004; Klepek *et al.*, 2005; Conde *et al.*, 2007a; Juchaux-Cachau *et al.*, 2007; Pommerrenig *et al.*, 2007). This feature of VvPLT1 led to a more detailed investigation of this protein, from its phylogenetic analysis (Supplementary Fig. S5 at JXB online) and molecular cloning to the demonstration of its functional and physiological role in grapevine. The polyol transporter VvPLT1 displayed only 50–59% sequence identity with the other putative VvPLTs (Supplementary Table S1), making this polyol transporter somewhat different from other grapevine polyol transporters. The order VvPLT2 to VvPLT5 that was established in Supplementary Table S1 was based on the sequence identity decrease relative to VvPLT1. An analysis using PLACE (Higo *et al.*, 1999) on the promoter sequence of VvPLT1 revealed the existence of several abiotic stress-related *cis*-acting elements, such as MYCCONSENSUSAT, with a significant number of identified copies (Supplementary Table S2).

The grapevine *VvMTD1* (*Vitis vinifera* NAD⁺-dependent mannitol dehydrogenase 1) was also cloned from the pulp of mature grape berries, and *in silico* and phylogenetic analyses of the amino acid sequence of this cytosolic mannitol dehydrogenase showed high similarities with polyol dehydrogenases from other plants (Supplementary Figs S6, S7 at JXB online). Like *VvPLT1*, several abiotic stress-related *cis*-acting elements were identified in the promoter sequences of *VvMTD1* (Supplementary Table S3). Further *in silico*

analysis, using NetPhos 2.0 (Blom *et al.*, 1999) revealed several serine, threonine, and tyrosine putative phosphorylation sites in the VvMTD1 amino acid sequence, suggesting that post-translational phosphorylation/dephosphorylation events are a possible regulatory mechanism of VvMTD1 mannitol oxidation activity (Supplementary Fig. S6).

Functional characterization of VvPLT1 by heterologous expression in S. cerevisiae

To demonstrate the function of VvPLT1 as a plasma membrane polyol transporter, the yeast strain MaDH4 was transformed with the vector pYES-DEST52 containing the VvPLT1 cDNA obtained from the grape berry pulp, under the control of the galactose-inducible GAL1 promoter. Yeast cells expressing VvPLT1 were clearly able to transport D-[¹⁴C]mannitol at a much higher rate than control cells

(pYES-DEST52 without VvPLT1), and the initial uptake rates of 0.2–20 mM mannitol followed Michaelis–Menten kinetics, indicating carrier-mediated transport. The following kinetic parameters were obtained for mannitol transport via VvPLT1: K_m , 5.4 mM mannitol; V_{max} , 0.37 nmol mannitol $min^{-1} mg^{-1} DW$ (Fig. 6A). The uptake of D-[¹⁴C]mannitol, at pH 4.5, was strongly inhibited (80%) by 50 μM of the protonophore CCCP, indicating H⁺-dependent active transport (Fig. 6B).

To determine the substrate specificity of VvPLT1, the uptake of 5 mM D-[¹⁴C]mannitol was examined in the presence of other putative competitors at a 10-fold higher external concentration (Fig. 6C). Other polyols, including dulcitol (82%), sorbitol (47%), galactinol (44%), and the cyclic polyol myo-inositol (30%), inhibited the VvPLT1-mediated uptake of D-[¹⁴C]mannitol, supporting the notion of VvPLT1 functioning as a broader polyol transporter. Basal D-[¹⁴C]mannitol uptake rates not mediated by VvPLT1 measured in control MaDH4 cells containing only the empty vector were

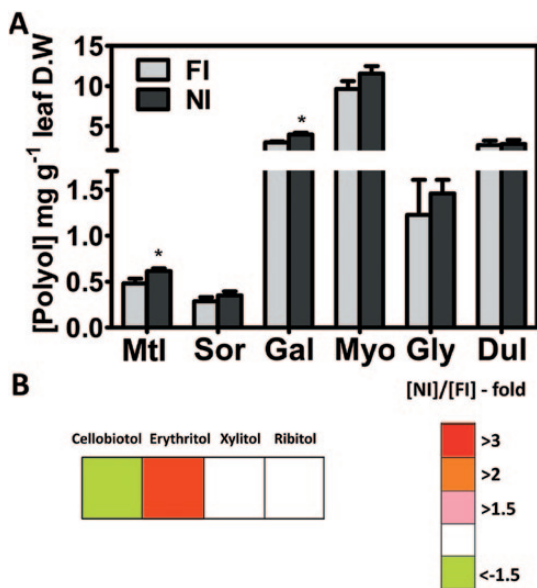


Fig. 3. Effect of water-deficit stress on the accumulation of polyols in grape leaves. (A) Concentrations of mannitol, sorbitol, galactinol, myo-inositol, glycerol, and dulcitol in leaves from fully irrigated (FI leaves) and non-irrigated (during 4 weeks) potted grapevines (NI leaves). An asterisk indicates statistical significance (Student’s *t*-test; $P < 0.05$). (B) Relative amounts of cellobiotol, erythritol, xylitol, and ribitol in NI leaves relative to FI leaves (fold variation). Metabolomic analysis was performed by GC-TOF-MS. Values are the mean \pm SEM of three experiments.

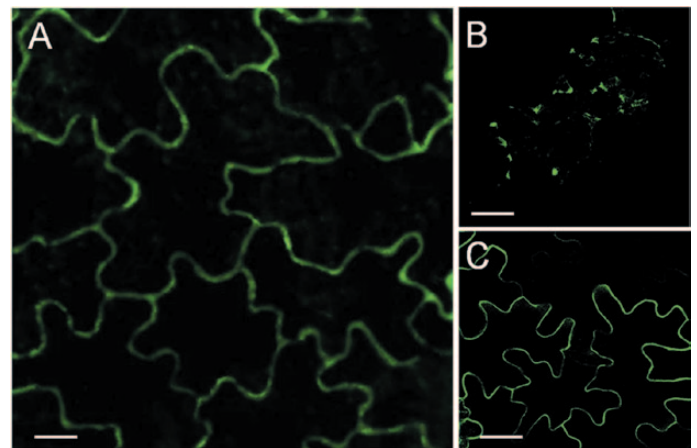


Fig. 5. VvPLT1-GFP localizes to the plasma membrane, as observed by confocal microscopy. (A) GFP fluorescence signal in the periphery of tobacco cells, localized in the plasma membrane, which only occurs in tobacco leaf epidermis cells transiently expressing VvPLT1-GFP. Scale bar=10 μm . (B) Diffuse GFP fluorescence signal of tobacco leaf epidermis cells transiently expressing GFP only (empty p7FWG2.0 plasmid), as a negative control. Scale bar=20 μm . (C) Fluorescence signal of the transient expression of the plasma membrane marker AtPIP1;4-YFP at the periphery of tobacco cells, localized in the plasma membrane, as a positive control. Scale bar=20 μm .

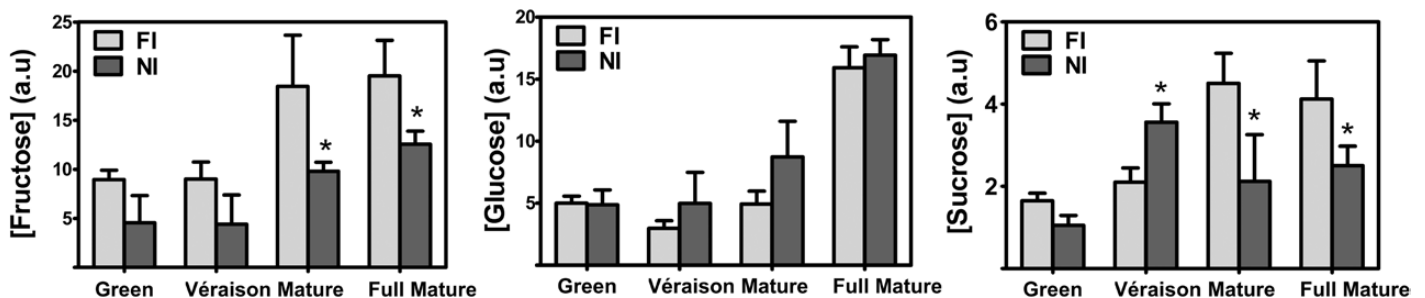


Fig. 4. Effect of water-deficit stress on the accumulation of glucose, fructose, and sucrose in grape berries. Relative amounts (in arbitrary units; a.u.) of fructose, glucose, and sucrose in grape berry mesocarps at different developmental stages in vines subjected to different irrigation regimes (FI, full irrigation; NI, non-irrigation). Metabolomic analysis was performed by GC-TOF-MS. Values are the mean \pm SEM of three experiments. An asterisk indicates statistical significance (Student’s *t*-test; $P < 0.05$).

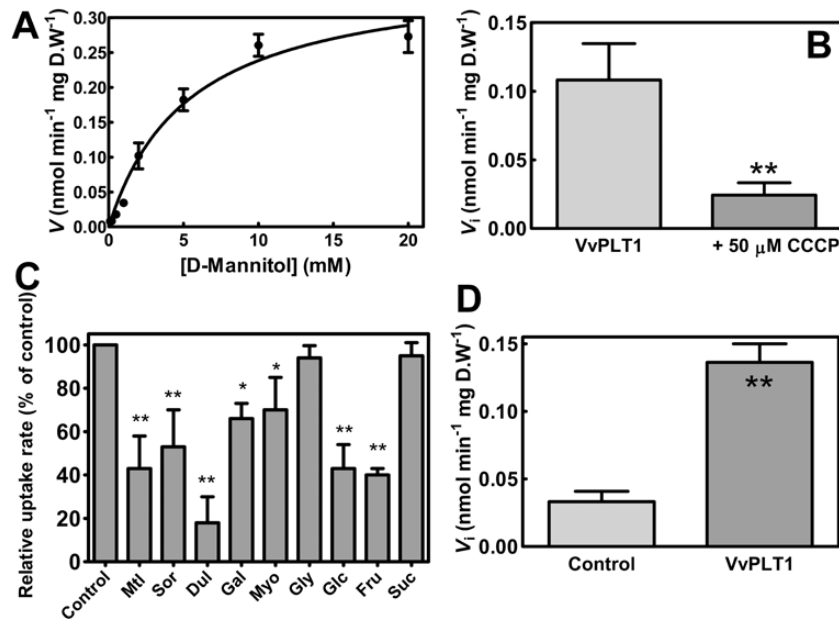


Fig. 6. Mannitol transport in *S. cerevisiae* MaDH4 cells heterologously expressing *VvPLT1*. Yeast cells were grown until early exponential phase in minimal medium supplemented with 2% galactose to induce the expression of *VvPLT1*, which is under the control of the galactose-inducible promoter GAL1 of the plasmid pYES-DEST52. (A) Concentration dependence of the initial uptake rates of D-[¹⁴C]mannitol in *VvPLT1*-expressing MaDH4 cells, at pH 4.5. Mannitol transport rates of MaDH4 control cells (with the pYES-DEST52 plasmid without *VvPLT1*) were subtracted from mannitol uptake rates from *VvPLT1*-expressing cells to determine the *VvPLT1*-dependent mannitol transport rates at various mannitol concentrations. (B) Effect of 50 μM of the protonophore CCCP on the *VvPLT1*-dependent uptake of 2 mM D-[¹⁴C]mannitol. (C) Specificity of the *VvPLT1* polyol transporter. Mannitol, sorbitol, galactinol, dulcitol, *myo*-inositol, glycerol, glucose, fructose, and sucrose at a concentration of 50 mM were added immediately before the addition of 5 mM of radiolabelled mannitol. All values depict the *VvPLT1*-dependent uptake of radiolabelled mannitol. (D) Initial uptake rates of 2 mM D-[¹⁴C]mannitol in control (transformed with the pYES-DEST52 plasmid without *VvPLT1*) and *VvPLT1*-expressing MaDH4 yeast cells. The duration of all uptake experiments was 2 min. All values are the mean ± SEM of three independent uptake experiments, except in (C) where values are the mean ± SEM of two independent uptake experiments. Asterisks indicate statistical significance (Student's *t*-test; **P*<0.05; ***P*<0.01).

approximately a quarter of the D-[¹⁴C]mannitol uptake rates of *VvPLT1*-expressing cells (Fig. 6D). In addition, *VvPLT1* also transported D-[¹⁴C]sorbitol following Michaelis–Menten kinetics with a K_m of 9.5 mM sorbitol. A clear inhibition of D-[¹⁴C]sorbitol uptake was obtained with 50 mM unlabelled mannitol (Supplementary Fig. S8A at JXB online), further confirming that they share the same carrier. Basal D-[¹⁴C]sorbitol uptake rates not mediated by *VvPLT1* were approximately a third of those of *VvPLT1*-expressing cells (Supplementary Fig. S8B). Glycerol, a 3-C polyol, did not inhibit mannitol uptake, thus evidencing that it is not transported by this plasma membrane carrier. Monosaccharides such as glucose and fructose also reduced mannitol uptake by *VvPLT1* (57% and 60%, respectively), suggesting that some monosaccharides may be transported by this carrier, similarly to *AtPLT5* of *Arabidopsis* (Klepek *et al.*, 2005). Sucrose had no influence on the transport rates of mannitol via *VvPLT1*. Indeed, *VvPLT1* was also capable of transporting the non-metabolizing glucose analogue 3-*O*-methyl-D-[U-¹⁴C]glucose, but with a much lower affinity (K_m of 28.5 mM) than mannitol (Supplementary Fig. S9).

Overall, the functional studies on *VvPLT1* clearly demonstrated the operation of an H⁺-dependent polyol transport system in grapevine.

Polyols had a protective effect in CSB grapevine cells

CSB cells were cultivated in the absence or presence of 100 mM NaCl and 15% (w/v) PEG 8000 (that induces the same water

potential as 100 mM NaCl; see the Materials and methods) up to the end of the exponential phase. Mannitol and sorbitol clearly protected salt- and osmotic-stressed CSB cells. The cytotoxic effect, represented by a decrease of the final biomass (DW) by salinity (NaCl) and osmotic stress (PEG), was higher in CSB cells cultivated with 1% (w/v) glucose than in cells cultivated with 0.5% (w/v) glucose+0.5% (w/v) mannitol or 0.5% (w/v) glucose+sorbitol 0.5% (w/v) (Fig. 7A, 7B). Treatments with NaCl and PEG for 24 h increased by almost 2- and 1.5-fold, respectively, the saturable transport rates of D-[¹⁴C]mannitol in grapevine cells cultivated in a medium with glucose and mannitol (Fig. 7C).

The first step of mannitol catabolism in grapevine is catalysed by *VvMTD*, encoded by *VvMTD1*. A biochemical characterization of grapevine mannitol dehydrogenase activity, performed in crude protein extracts of grape cells cultivated with glucose+mannaol, followed Michaelis–Menten kinetics with a K_m of 30.1 mM mannitol and a V_{max} of 0.63 μmol h⁻¹ mg protein⁻¹ (Fig. 7D). The V_{max} estimated in glucose-grown cells in the absence of the polyol was 70% less than in the presence of mannitol in the culture medium (Fig. 7E). In a diametrically opposite manner to mannitol uptake, the mannitol oxidation rate was strongly repressed by 24 h treatments with 100 mM NaCl in cells grown with glucose+mannaol (Fig. 7E). HPLC analysis confirmed that mannitol accumulated intracellularly in salt-stressed cells (Fig. 7F). However, in PEG-treated cells the intracellular concentration of mannitol was roughly the same as that of the control. Moreover, the

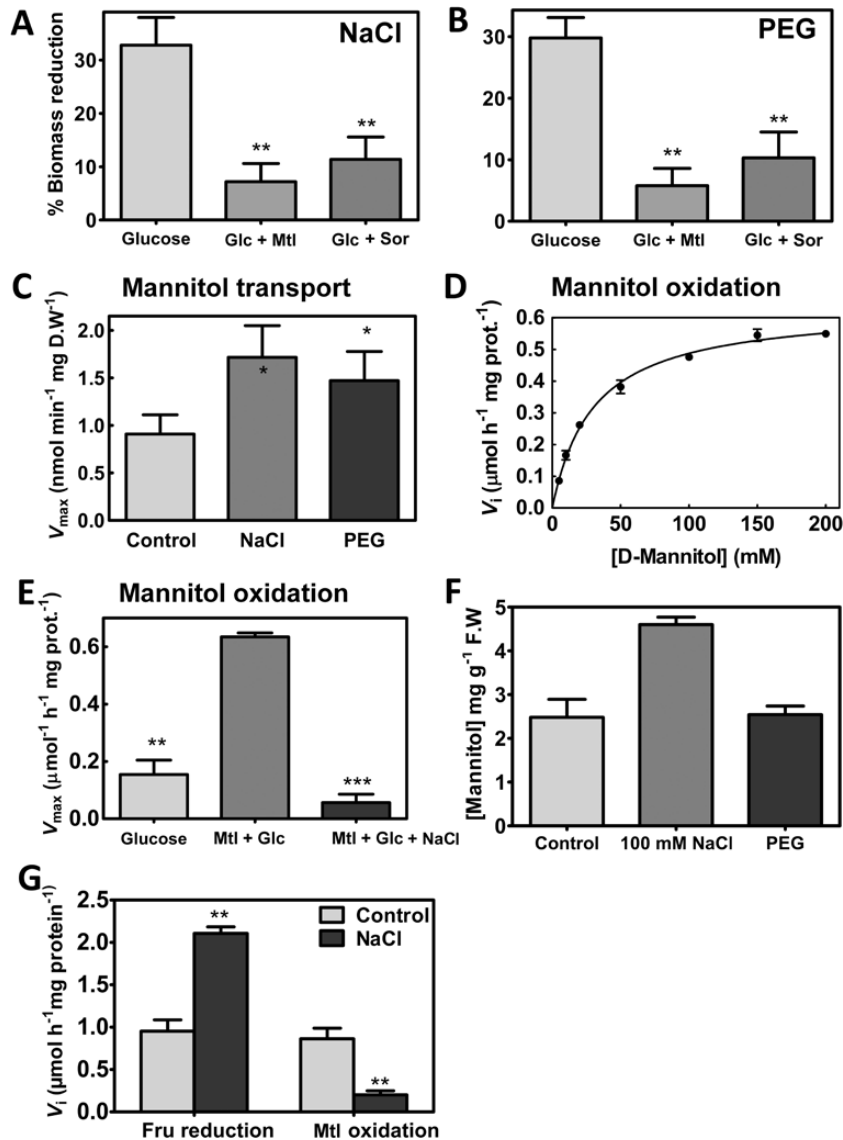


Fig. 7. Mannitol and sorbitol prevent the loss of biomass of grape cell cultures under osmotic 15% (w/v) PEG and salt (100 mM NaCl) stresses following transport capacity increase and catabolism repression. CSB suspension-cultured cells were grown up to the end of the exponential growth phase with 1% (w/v) glucose, 0.5% (w/v) glucose+0.5% (w/v) mannitol, or 0.5% (w/v) glucose+0.5% (w/v) sorbitol, in the presence or absence of 100 mM NaCl (A) or (w/v) PEG (B). The percentage biomass reduction is relative to the control. (C) Salt (100 mM NaCl) and osmotic stress (PEG) increases the V_{max} of D -[¹⁴C]mannitol uptake, at pH 4.5, in grape suspension-cultured cells cultivated with 0.5% (w/v) mannitol+0.5% (w/v) glucose collected at mid-exponential growth phase, after 24 h of treatment. (D) Michaelis–Menten kinetics of mannitol oxidation in CSB cells cultivated with 0.5% glucose+0.5% mannitol and harvested at mid-exponential growth phase. (E) The maximum rate of mannitol oxidation in cells cultivated with 0.5% (w/v) glucose+0.5% (w/v) mannitol is strongly repressed after 100 mM NaCl and 15% (w/v) PEG treatments for 24 h, at mid-exponential growth phase. Also in (E), the V_{max} of mannitol catabolism is much higher in cells cultivated in the presence of mannitol than in CSB cells cultivated with 1% glucose as the only carbon and energy source. (F) Effect of 100 mM NaCl and 15% (w/v) PEG stress on the intracellular accumulation of mannitol in CSB cells cultivated with 0.5% (w/v) glucose+0.5% (w/v) mannitol determined by HPLC analysis. (G) Salt stress-induced shift in the activity of $VvMTDs$ in CSB grapevine cells cultivated with 0.5% (w/v) glucose+0.5% (w/v) mannitol. The effect of 100 mM NaCl on the initial velocity of 200 mM fructose reduction or 200 mM mannitol oxidation. All values represent the mean \pm SEM of three independent experiments. Asterisks indicate statistical significance (Student's t -test; * P <0.05; ** P <0.01; *** P <0.001).

treatment with NaCl doubled the fructose reduction activity of $VvMTD$ and repressed the reverse reaction of mannitol oxidation (Fig. 7G).

Gene expression analysis by qPCR studies in glucose-grown CSB cells showed that salt stress and water-deficit stress triggered a 3- and 2-fold increase, respectively, in $VvPLTI$ transcripts (Fig. 8A). The expression of $VvPLTI$ was also significantly increased by ABA, a key abiotic stress signalling molecule, and salicylic acid (SA). The expression

of $VvPLTI$ was higher (2.5-fold) in grapevine cells cultivated in the presence of mannitol and glucose, suggesting an increase in $VvPLTI$ transcripts caused by its own substrate (Fig. 8B). Similarly to what was observed in glucose-grown cells, salt and osmotic stress also increased the steady-state transcript abundance of $VvPLTI$ in cells grown in the presence of mannitol by 4-fold and a 2- to 3-fold, respectively (Fig. 8C). Also, $VvMTD1$ expression was strongly stimulated by NaCl and PEG treatments (almost 80- and 30-fold,

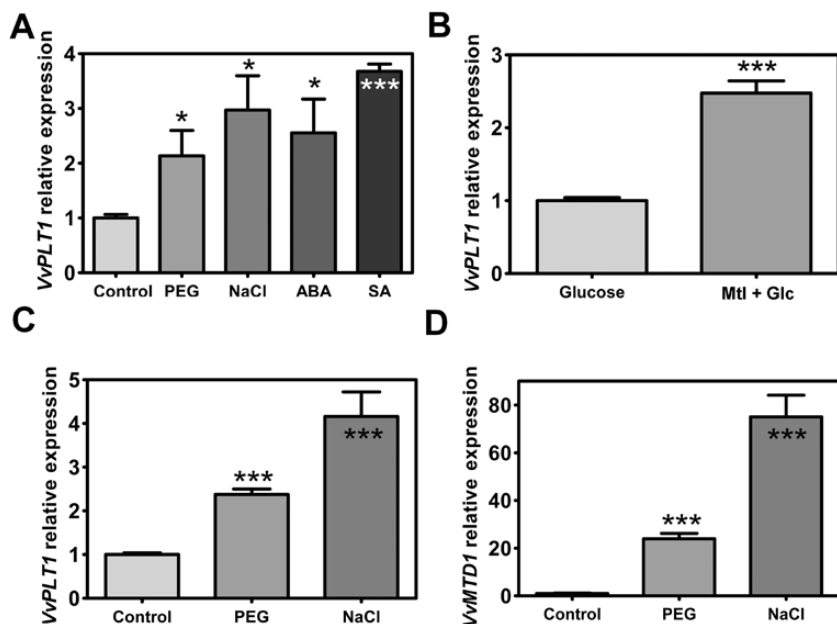


Fig. 8. *VvPLT1* and *VvMTD1* gene expression analysis in CSB grape cells by real-time qPCR. (A) The effect of 24 h treatments with 100 mM NaCl, 15% (w/v) PEG, 150 μ M ABA, and 50 μ M SA on *VvPLT1* expression in CSB cells cultivated with 1% (w/v) glucose. (B) *VvPLT1* expression in CSB cells cultivated in the presence of 1% glucose versus 0.5% (w/v) mannitol+0.5% (w/v) glucose. (C) The effect of 24 h treatments with 100 mM NaCl and 15% (w/v) PEG on *VvPLT1* expression on cells cultivated with 0.5% (w/v) mannitol+0.5% (w/v) glucose. (D) The effect of 24 h treatments with 100 mM NaCl and 15% (w/v) PEG on *VvMTD1* expression on cells cultivated with 0.5% (w/v) mannitol+0.5% (w/v) glucose. *VvPLT1* and *VvMTD1* relative expression levels were obtained after normalization with the expression of the reference genes *VvACT1* and *VvGAPDH*. Three independent qPCR experiments, one for each biological replicate, with duplicates were performed for each tested mRNA. Values are the mean \pm SEM. Asterisks indicate statistical significance (Student's *t*-test; **P*<0.05; ****P*<0.001).

respectively) in grapevine cells cultivated with polyols and glucose (Fig. 8D).

Water-deficit stress regulated the biochemical activity of MTD and SDH, and the expression of VvPLT1, VvMTD1, and VvSDH1 in the grape berry

To assess the metabolic changes that allow grape berry tissues to accumulate polyols, such as mannitol and sorbitol, in response to water-deficit stress, the total activity of *VvMTDs* and *VvSDHs* was measured in the pulp tissue of water deficit-stressed (NI) and FI berries at each berry developmental stage. The catabolism of mannitol followed Michaelis–Menten kinetics with a K_m of 79 ± 24 mM mannitol, which is higher than that of CSB cells (Fig. 9D). The biochemical activity of both enzyme types increased steadily during ripening in berries of both fully irrigated and water deficit-stressed vines, reaching maximum rates at the fully mature stage: $4.5 \mu\text{mol h}^{-1} \text{mg protein}^{-1}$ for mannitol oxidation and $2.7 \mu\text{mol h}^{-1} \text{mg protein}^{-1}$ for sorbitol oxidation in the pulp of FI berries (Fig. 9A, B). However, both mannitol and sorbitol oxidation was strongly inhibited in water-deficit-stressed grape berries, particularly in the later ripening stages, where only 25% of the *VvMTD* and 50% of *VvSDH* activities of well-watered plants was measured in NI berries (Fig. 9A, B). Moreover, in fully mature grape berries, when maximum mannitol oxidation rates were observed, in the pulp tissues from NI berries, in addition to the strong inhibition of *VvMTD*-mediated mannitol oxidation, there was a significant stimulation of the reverse reaction towards mannitol

biosynthesis (Fig. 9C). A remarkable 5-fold up-regulation of fructose reduction was observed in the pulp of fully mature berries of water deficit-stressed grapevines when compared with FI conditions. Using the same concentration of fructose or mannitol (200 mM), in FI the preferred reaction catalysed by *VvMTDs* was undoubtedly the oxidation of mannitol into fructose, whereas, under water-deficit conditions, the reverse reaction was clearly favoured, with a fructose reduction rate much higher than the oxidation of mannitol.

While the catabolism of polyols such as mannitol and sorbitol was clearly inhibited in the pulp of fully mature grape berries of water-deficit-stressed vines, the polyol transporter *VvPLT1* gene expression was increased by 2.5-fold in response to water deficit (Fig. 10). Conversely, *VvMTD1* and *VvSDH1* transcripts were only 20% and 40% inferior in fully mature NI berries when compared with FI conditions. Notably, this down-regulation was less pronounced than the observed inhibition of mannitol and sorbitol oxidation activity. However, *VvMTD1* and *VvSDH1* transcript abundance was slightly higher in NI berries when compared with FI at the green berry stage, the same stage at which *VvPLT1* steady-state transcript abundance was the highest in berries from well-watered vines. Nevertheless, the coordination between an overexpression of *VvPLT1* and a slight under-expression of both polyol dehydrogenase genes under water-deficit conditions was seen in the final maturation stages of the grape berry, immediately before harvest. Also, abundant steady-state transcripts of *VvPLT1* were detected by qPCR in mesophyll tissues of mature leaves from potted grapevines (Supplementary Fig. S10 at JXB online) suggesting, together

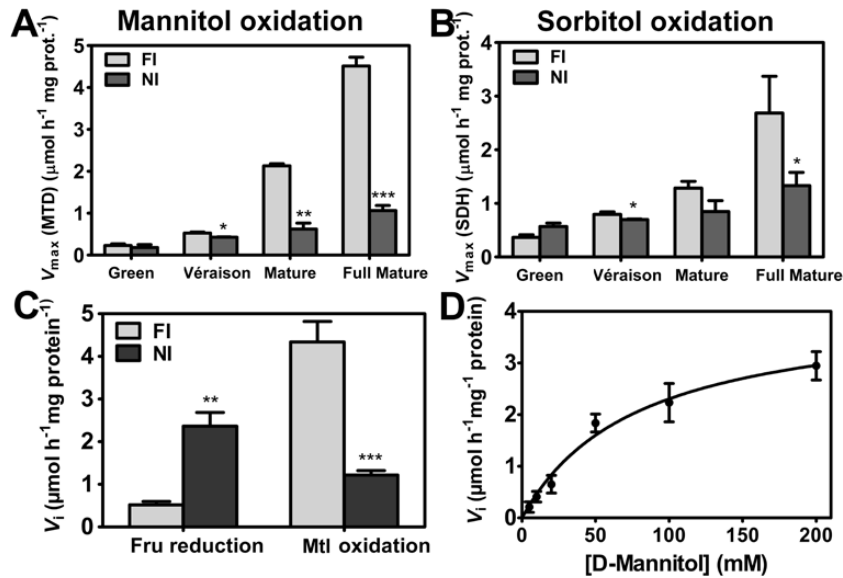


Fig. 9. Water-deficit stress regulates the biochemical activity of VvMTD and VvSDH in grape berries. V_{max} of mannitol (A) and sorbitol (B) oxidation in grape berry mesocarps at different developmental stages in vines subjected to different irrigation regimes (FI, full irrigation; NI, non-irrigation) shows that drought inhibits mannitol and sorbitol oxidation. Values are the mean \pm SEM of three independent experiments. (C) Water-deficit stress-induced shift in the activity of VvMTD in pulp tissues of fully mature grape berries. The effect of drought stress (NI) on the initial velocity of 200 mM fructose reduction or 200 mM mannitol oxidation via VvMTD. Values are the mean \pm SEM of three independent experiments. (D) Michaelis–Menten kinetics of mannitol oxidation in pulp tissues of fully mature grape berries. Values are the mean \pm SEM of two independent experiments. Asterisks indicate statistical significance (Student's *t*-test; * $P < 0.05$; ** $P < 0.01$; *** $P < 0.001$).

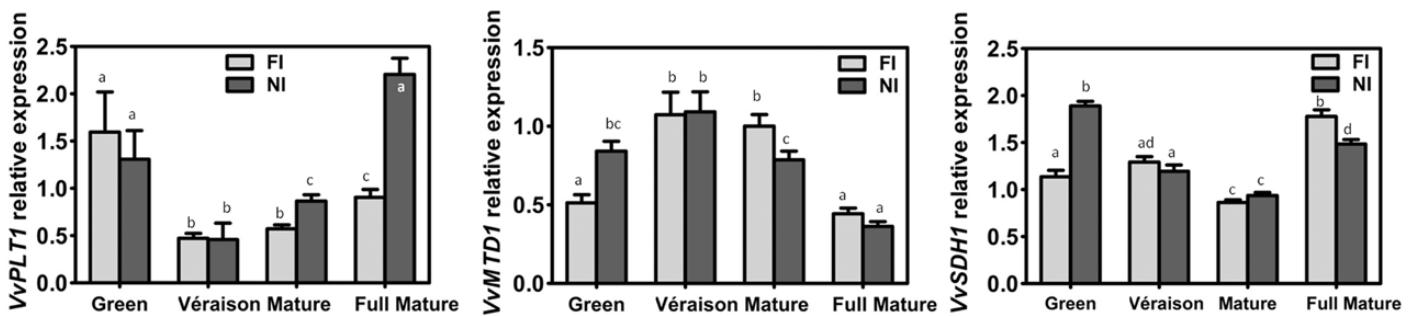


Fig. 10. The effect of water-deficit stress on the transcript abundance of *VvPLT1*, *VvMTD1*, and *VvSDH1* in grape berries. Relative gene expression analysis, by real-time qPCR, of *VvPLT1*, *VvMTD1*, and *VvSDH1* in grape berry mesocarps at different developmental stages in vines subjected to different irrigation regimes (FI, full irrigation; NI, non-irrigation). *VvPLT1*, *VvMTD1*, and *VvSDH1* relative expression levels were obtained after normalization with the expression of the reference genes *VvACT1* and *VvGAPDH*. Three independent qPCR experiments, one for each biological replicate, with duplicates were performed for each tested mRNA. Values are the mean \pm SEM. For each gene, columns sharing the same letter are not significantly different (two-way ANOVA with Tukey's post-test).

with the considerable concentration of polyols detected, that it could play a role in exporting polyols/monosaccharides from leaves that could ultimately be taken up by sink cells at higher rates in water-deficit conditions.

Discussion

Polyol accumulation in grape berries as a response mechanism against water-deficit stress

Water-deficit stress stimulated the accumulation of the majority of the quantified polyols in the pulp of grape berries from field-grown grapevines (cv. Tempranillo), suggesting that grape berries use polyols as effective osmoprotectants to maintain cell and tissue homeostasis.

The concentration of mannitol in fully mature grape berries from water-deficit-stressed plants is very relevant ($2 \text{ mg g}^{-1} \text{ DW}$) because it falls within the concentration range found in fruits of some well-known polyol-producing plants. For instance, in the mannitol-synthesizing species *O. europaea*, mannitol reaches $8 \text{ mg g}^{-1} \text{ DW}$ in mature olives (Marsilio *et al.*, 2001). Similarly to mannitol, a strong accumulation of sorbitol ($3 \text{ mg g}^{-1} \text{ DW}$), galactinol ($1.8 \text{ mg g}^{-1} \text{ DW}$), myo-inositol ($6.5 \text{ mg g}^{-1} \text{ DW}$), dulcitol ($4.2 \text{ mg g}^{-1} \text{ DW}$), and less common polyols such as cellobiotol, erythritol, and xylitol in grape berry pulp tissue was also triggered by water deficit. The total concentration of polyols in water-deficit-stressed plants reached up to $20 \text{ mg g}^{-1} \text{ DW}$, in contrast to the much lower total of $8 \text{ mg g}^{-1} \text{ DW}$ in well-watered plants. This is very significant because this concentration was slightly higher

than the concentration of sucrose, a major grapevine photoassimilate, in the pulp of normal Cabernet Sauvignon mature grape berries (Pillet *et al.*, 2012) and ~15% of the glucose and 12% of fructose concentrations found at the same maturation stages. It was, in fact, greater than the 15 mg g⁻¹ DW of sucrose in Tempranillo FI mature berries, the irrigation treatment displaying the highest sucrose concentration, determined in a parallel HPLC analysis (Supplementary Fig. S11 at *JXB* online). Taking into account that water deficit causes a decrease in berry size (Conde *et al.*, 2007b), the relative accumulation of polyols in water deficit-stressed plants would be even more accentuated if on a fresh weight basis.

Galactinol, present in the grape berry at higher concentrations until the early mature stage of berry development, has already been shown to contribute to the heat stress resistance process of Cabernet Sauvignon grapevines, where the expression of a galactinol synthase (VvGOLS1) was increased by high temperature stress (Pillet *et al.*, 2012). Undetected in unstressed Cabernet Sauvignon grape berries, the concentration of galactinol increased up to 0.3 mg g⁻¹ DW and 0.4 mg g⁻¹ DW in the pulp and skin, respectively, of heat-stressed mature grape berries. However, these values are lower than the 1.8 mg g⁻¹ DW and 0.9 mg g⁻¹ DW revealed in the pulp of mature and fully mature Tempranillo water-deficit-stressed grape berries (this study). Heat stress and water deficit are two tightly related abiotic stresses, as high temperatures often provoke low water soil contents. In agreement with this, the steady-state transcript abundance of a galactinol synthase had already been shown to increase significantly in shoot tips of water- and salt-stressed Cabernet Sauvignon grapevines (Cramer *et al.*, 2007; Tattersall *et al.*, 2007). Galactinol is also an intermediary in the synthesis of raffinose, a carbohydrate with a protective role against water and abiotic stress-induced oxidative stress in several plant species (Nishizawa *et al.*, 2008). Therefore, in addition to acting as an osmoprotective compound, the accumulation of galactinol may also be advantageous for an increased raffinose production as a defensive mechanism against water deficit. However, raffinose was not unequivocally detected in the present metabolomic analysis, making it impossible to determine any association with the concentration of galactinol.

Myo-inositol is an important cellular metabolite that forms the structural basis of several lipid signalling molecules that act in diverse pathways, including environmental stress responses, plasma membrane biogenesis, the regulation of cell death, auxin perception, cell wall biosynthesis, and synthesis of ascorbic acid (Ishitani *et al.*, 1996; Nelson *et al.*, 1998; Meng *et al.*, 2009; Donahue *et al.*, 2010). In some plants, *myo*-inositol is also a compatible osmolyte that protects cells from salinity and osmotic stress-induced damage, but its derivatives pinitol or ononitol can also be accumulated to high concentrations as osmolytes (Thomas and Bohnert, 1993; Sheveleva *et al.*, 1997; Nelson *et al.*, 1998). However, in other species, such as *Arabidopsis*, increased *myo*-inositol concentrations reflect a higher demand for galactinol, as salinity or osmotic stress result in enhanced synthesis of its derivative raffinose (Taji *et al.*, 2002). In the present study, an increase in *myo*-inositol concentration

appears to be strategy of grape berry tissues to cope with water deficit, either directly as an osmolyte or indirectly as a precursor of galactinol and raffinose family oligosaccharides. In agreement with a role for *myo*-inositol as an osmolyte in grapevine, the steady-state transcript abundance of *myo*-inositol-1-phosphate synthase, the first enzyme in the *myo*-inositol biosynthesis pathway, was strongly stimulated (>2-fold) as rapidly as 4 h after a period of stress due to water deficit and salinity in shoot tips of Cabernet Sauvignon (Tattersall *et al.*, 2007).

In contrast, the concentration of glycerol followed an opposite trend under water deficit, suggesting that it is not an osmolyte in grapevine. This polyol is different from all polyols accumulated upon water deficit, with its 3-C backbone structure and greater water binding capacity and role as a precursor of membrane phospholipids.

In mature leaves, measurable concentrations of several polyols in grapevine mesophyll cells (including mannitol and sorbitol) might indicate their biosynthesis in this source tissue, similarly to other polyol-accumulating plant species including *P. major* (Pommerrenig *et al.*, 2007). In agreement with this, even though the increase in mannitol and sorbitol concentrations was not pronounced, the gene expression of a putative grapevine aldose reductase [whose sequence was retrieved from the Genoscope Genome Browser (12X), Jaillon *et al.*, 2007] with strong homology with sorbitol-6-phosphate dehydrogenases (74%) and mannose-6-phosphate reductases (88%)—enzymes involved in sorbitol and mannitol biosynthesis in other polyol-producing plants—increased 70% under water deficit (Supplementary Fig. S12 at *JXB* online). This is somewhat similar to the case of peach (*Prunus persica*), where the *in vitro* activity of an aldose-6-phosphate reductase, the key enzyme in sorbitol synthesis, increased in response to water deficit, as did the partitioning of newly fixed carbon into sorbitol and its export and quantity in the phloem sap (Escobar-Gutiérrez *et al.*, 1998).

VvPLT1 is a grapevine polyol transporter with a broad specificity

The molecular characterization of VvPLT1 showed that the amino acid sequence of this MFS member polyol transporter is somewhat divergent from that of the other four predicted PLTs (50–59% identity) and is the grapevine polyol transporter, sharing higher homology with already characterized functional plasma membrane polyol transporters from other plants. A sequence in the grapevine genome highly similar to Tempranillo VvPLT1 had been briefly referred to in the literature for the cultivar Chardonnay (Afoufa-Bastien *et al.*, 2010) by the name of VvPMT5, after *in silico* homology was inferred in the Genoscope Genome Browser (Jaillon *et al.*, 2007). VvPMT5 was described as a possible polyol/monosaccharide transporter due to its strong homology with the *Arabidopsis* polyol/monosaccharide transporter AtPLT5. However, because this carrier has higher affinity for polyols than for monosaccharides and the acronym PLT has been used for the majority of plant polyol transporters (even for those also transporting monosaccharides), the acronym PLT

was also used here. The presence in the promoter of *VvPLT1* of numerous copies of several abiotic stress-related *cis*-acting elements, such as MYCCONSENSUSAT, clearly suggests transcriptional regulation of *VvPLT1* expression by environmental challenges. In addition to being responsive to water deficit and dehydration, a large number of copies of *cis*-acting elements related to other stresses such as salt, cold, and excess light, to abiotic stress signalling by ABA and SA, and responsive to biotic stress were also identified (entry Table S2 at *JXB* online).

VvPLT1 is an H⁺-dependent polyol transporter with high affinity for sorbitol and mannitol. However, competitive inhibition studies suggested that other polyols and even monosaccharides might share this plasma membrane transporter with lower affinities. Like many other polyol transporters, *VvPLT1* appears to have a low substrate specificity. The affinities of *VvPLT1*-mediated D-[¹⁴C]mannitol (K_m , 5.4 mM) and D-[¹⁴C]sorbitol (K_m , 9.5 mM) uptake were well in line with the polyol affinity range characterized in several polyol transporters from other plants, including apple (3.2 mM sorbitol for MdSOT5), *P. major* (12 mM and 20 mM sorbitol for PmPLT1 and PmPLT2), and *O. europaea* (1.8 mM mannitol for OeMaT1) (Ramsperger-Gleixner *et al.*, 2004; Watari *et al.*, 2004; Conde *et al.*, 2007a), but lower than those of sour cherry (0.64 mM and 0.82 mM sorbitol for PcSOT1 and PcSOT2) and celery (0.34 mM and 1.8 mM mannitol for AgMaT1 and AgMaT2) (Noiraud *et al.*, 2001a; Gao *et al.*, 2003; Juchaux-Cachau *et al.*, 2007). In the non-transporting species *Arabidopsis*, the K_m value of AtPLT5 for sorbitol is 0.5 mM, with an inferior affinity for glucose and other monosaccharides (Klepek *et al.*, 2005); and 0.77 mM sorbitol for AtPMT1, a broad range polyol/monosaccharide transporter (Klepek *et al.*, 2010). Monosaccharides such as glucose and fructose inhibited the *VvPLT1*-mediated transport of mannitol and sorbitol, and the non-metabolizing glucose analogue 3-*O*-methyl-D-glucose was also transported in an H⁺-dependent manner, suggesting that this carrier might function as a polyol/monosaccharide carrier, similarly to the biochemical function of AtPLT5 (Klepek *et al.*, 2005; Reinders *et al.*, 2005) or AtPMT1 and AtPMT2 (Klepek *et al.*, 2010). In celery, however, fructose and particularly glucose, interestingly both sugars stored in the parenchyma of celery petioles, were highly inhibitory of mannitol uptake via AgMaT1 and AgMaT2 even though no significant radiolabelled glucose transport mediated by these transporters was detected (Noiraud *et al.*, 2001a; Juchaux-Cachau *et al.*, 2007).

VvMTD1 encodes a grapevine mannitol dehydrogenase with oxireductase activity and is under regulation of abiotic stress-related *cis*-acting elements

The grapevine *VvMTD1* was also cloned from the pulp of mature grape berries and the amino acid sequence of its encoded protein shares strong homology with polyol dehydrogenases from other plants. The oxireductase activity of the cytosolic enzyme encoded by *VvMTD1* is a key step in the metabolism of mannitol because it catalyses the first step of its oxidation, in a reversible but predominant reaction where a

molecule of fructose is formed. Remarkably, an *in silico* analysis in UniProtKB/TrEMBL and Genoscope Genome Browser (12X) (Jaillon *et al.*, 2007) indicated the existence of 14 other probable *VvMTD*-like proteins with ≥80% sequence similarity, including three probable *VvMTDs* with ≥97% amino acid sequence similarity. Like *VvPLT1*, the promoter of *VvMTD1* also possesses several abiotic stress-related *cis*-acting regulatory elements, but with less variety and with a lower copy number, suggesting either positive or negative transcriptional regulation. Notably, one element, GT1CONSENSUS, a regulatory element involved in a positive and up-regulatory SA response, was by far the most abundant *cis*-acting element at the promoter of *VvMTD1*, with 24 copies. SA is a molecule involved in biotic stress signalling, and the expression of *MTDs* has already been found to be up-regulated during plant infection by several pathogens (Jennings *et al.*, 1998, 2002; Voegelé *et al.*, 2004).

Grapevine water-deficit stress tolerance provided by polyol accumulation in grape berries resulted from synergistic polyol transport and metabolism

At the cellular level (CSB cells), mannitol and sorbitol had a clear protective effect under salt (100 mM NaCl) and osmotic (15% PEG) stress. The mechanism behind this cellular protection appeared to be the co-ordination between a boosted polyol uptake and a strongly repressed oxidation coupled to a simultaneous stimulation of fructose reduction into polyols, allowing their intracellular accumulation. Sorbitol, similarly to mannitol, significantly diminished the stress-induced biomass reduction of grapevine cells, suggesting that they share the same cell strategy towards intracellular accumulation and osmoprotection. Mannitol and sorbitol are isomers with just a different orientation of the hydroxyl group of the second carbon. Mannitol is an efficient scavenger of hydroxyl radicals that result from abiotic stresses such as salinity and water deficit (Shen *et al.*, 1997a, b). In plants, the antioxidant function of mannitol may be to protect susceptible thiol-regulated enzymes such as phosphoribulokinase, ferredoxin, thioredoxin, and glutathione from inactivation by hydroxyl radicals (Shen *et al.*, 1997b). Thus, the accumulation of mannitol may have dual functions: providing osmotic adjustment and supporting redox control (Shen *et al.*, 1999). In grape cells, the role of mannitol and sorbitol in salt or osmotic stress cell tolerance as compatible solutes with an additional function as osmoprotectants against oxidative damage is perfectly plausible. In fact, in the mannitol-accumulating transgenic wheat, the majority of the protective effect of mannitol was mediated by the scavenging of hydroxyl radicals and stabilization of macromolecules (Abebe *et al.*, 2003). Also, photosystem II was less affected by salinity in persimmon trees that accumulated sorbitol by overexpression of sorbitol-6-phosphate dehydrogenase (*S6PDH*) from apple (Gao *et al.*, 2001).

In grapevine CSB cells, the significant increase of *VvPLT1* transcripts in response to salt and osmotic stresses and the abiotic and biotic stress signalling molecules ABA and SA is in agreement with the several abiotic and biotic stress-related

cis-acting elements identified in the promoter region of *VvPLT1*, and account for the increased mannitol transport capacity observed in grapevine cells under salinity and water-deficit stress. *VvPLT1* gene expression was also regulated by its own substrates. Additionally, the strong stimulation of *VvMTD1* transcription by salt and osmotic stress was concordant with an increased rate of NADH-dependent fructose reduction into its product mannitol that was inherently linked to the concomitant strong decrease in the mannitol oxidation activity of this mannitol dehydrogenase in response to these stresses. The shift towards fructose reduction in salt-stressed cells may have been the reason behind the very strong increase (nearly 80-fold) of *VvMTD1* gene expression in salt-stressed CSB cells [~25-fold under osmotic (PEG) stress].

At the plant level, the severe repression of the total mannitol and sorbitol oxidation activity in the berry pulp induced by water-deficit stress, particularly in the later ripening stages, suggested a strategy to maintain cell and pulp tissue homeostasis in these conditions. However, the strong decrease of polyol oxidation activity could be explained only in part by the slight repression of gene expression; thus, post-transcriptional or post-translational regulation of *VvMTDs* and *VvSDHs* was very likely. As shown by MTD assays in fresh homogenates from mesocarp, part of the mechanism of water and salt stress resistance in grapevine might be the increase in fructose reduction into mannitol, in parallel with the noticeable mannitol oxidation inhibition, in line with what happened in CSB cells.

To date, polyol biosynthesis in sink tissues has been considered non-existent taking into account the inactive polyol biosynthetic pathways via aldose and aldose-6-phosphate reductases (Loescher and Everard, 1996); however, in the present study, the very significant alterations in total mannitol oxidation and fructose reduction rates under water-deficit stress may be in part responsible for a water deficit-responsive mannitol synthesis and increased concentrations of polyols in sink cells and mesocarp tissues of Tempranillo grape berries (Fig. 11). The intracellular NAD^+/NADH ratio and overall redox status may also play a role in regulating MTD activity and the predominant direction of the reaction for the adjustment to the physiological conditions. This defence mechanism of parallel mannitol oxidation inhibition/fructose reduction stimulation may account in part for the lower fructose concentrations of water-deficit-stressed grape berries and the higher mannitol concentration.

Measurements of the total mannitol oxidation rate in grape berries are the clear-cut result of the action of all MTD isoforms and all possible regulatory mechanisms, and are physiologically much more relevant than any transcriptional analysis of all *VvMTD*-like genes, thus reflecting more accurately the effect of water deficit on the metabolism of mannitol. The same might be applied to *VvSDH* and sorbitol oxidation rates. In grapevine, under normal conditions, sorbitol dehydrogenase catalyses the oxidation of a molecule of sorbitol to a molecule of fructose in an NAD^+ -dependent reaction, but the reverse reaction is also possible. The water-deficit stress-induced inhibition of sorbitol oxidation via *VvSDH* thus may in part be due to a shift in the preferred direction of the reaction due to

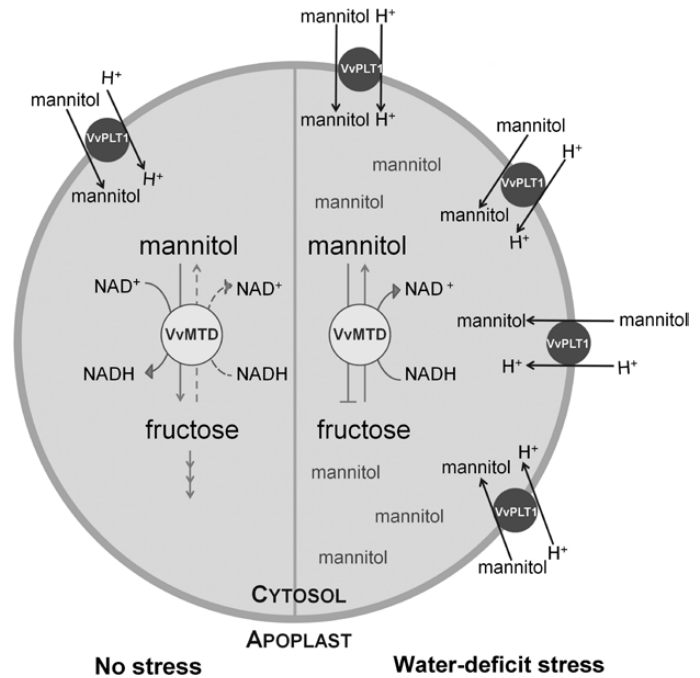


Fig. 11. Proposed model for a synergistic mechanism involving increasing mannitol transport and a shift in its metabolism towards a higher intracellular mannitol concentration as a defence mechanism of *V. vinifera* against salt/water-deficit stress at the cellular level.

post-translational regulation, regulation by the NAD^+/NADH ratio and/or by redox status, as suggested for MTDs.

The significant increase in the transcript abundance of *VvPLT1* (2.5-fold) in the mesocarp in response to water deficit-stress in the final stages of berry ripening is physiologically relevant, and it is similar to the salt-stress-induced 3- to 5-fold increase in the transcripts of *PmPLT1* and *PmPLT2* in the vascular tissue of common plantain (Pommerrenig *et al.*, 2007). Moreover, it was well in line with the 3-fold increase in the concentrations of several polyols such as mannitol and sorbitol, and the total concentration of polyols in fully mature berries in response to water deficit. The involvement of other *VvPLTs* in the accumulation of polyols cannot be ruled out. Nonetheless, the grapevine polyol transporter homologue to *VvPLT1* in Chardonnay was the most highly expressed *VvPLT* in most plant tissues, with a lower expression in grape berries (Afoufa-Bastien *et al.*, 2010). This suggests that the expression and availability of polyol transporters such as *VvPLT1* at the plasma membrane of pulp cells might be responsible for a limiting step or bottleneck in the uptake of sugar alcohols in these cells, and hence for its direct contribution to the water-deficit stress-induced accumulation of polyols.

However, the magnitude of response involving the synergistic *VvPLT1* overexpression and polyol dehydrogenase activity shift towards polyol accumulation in grape tissues upon water deficit may differ from cultivar to cultivar, as some varieties are better adapted to low water availability conditions than others. For instance, unlike in Tempranillo, significant amounts of mannitol or sorbitol were not detected in a parallel HPLC analysis on Touriga Nacional grape berries, a Portuguese grapevine variety less tolerant to water

deficit. The presence of a polyol, however, had already been detected in polar extracts of grape berries by [Deluc *et al.* \(2007\)](#) in Cabernet Sauvignon, but these authors were unable to distinguish whether it was sorbitol or mannitol; and sorbitol and *myo*-inositol were even detected in the phloem sap of Thompson Seedless grapevines ([Roubelakis-Angelakis and Kliewer, 1979](#)). Thus, edaphoclimatic conditions, the type and intensity of water/salt stress in combination with the genotype may influence the magnitude of the polyol metabolism changes and their accumulation.

In the context of the ongoing climate changes and its negative impacts ([Hannah *et al.*, 2013](#)), grapevine cultivars that accumulate polyols as a tolerance mechanism to water-deficit stress might be ideally adapted to these future environmental constraints, by requiring less water during viticultural practices to maintain grape productivity and berry quality. In agreement with this, the synthesis, transport, and accumulation of sugar alcohols offer considerable promise as bioindicators of plant health and acclimation, and as biomarkers used as selective traits for plant improvement ([Merchant and Richter, 2011](#)). Thus, the discovery of considerable amounts of polyols in grape berries in response to water-deficit stress, together with its genetic and molecular determinism, may have an important application in the improvement of grapevine practices and water use efficiency.

Supplementary data

Supplementary data are available at *JXB* online.

Figure S1. Heat map of the metabolome changes induced by water-deficit stress in grape berry mesocarps.

Figure S2. Heat map of the metabolome changes induced by water-deficit stress in grape leaves from potted vines.

Figure S3. Effect of water-deficit stress in the accumulation of fructose, glucose, and sucrose in grape leaves.

Figure S4. VvPLT1 amino acid sequence alignment and comparison with homologues from other plant species.

Figure S5. Phylogenetic analysis of VvPLT1.

Figure S6. VvMTD1 amino acid sequence alignment and comparison with homologues from other plant species.

Figure S7. Phylogenetic analysis of VvMTD1.

Figure S8. Sorbitol uptake in *S. cerevisiae* MaDH4 cells heterologously expressing *VvPLT1*.

Figure S9. Glucose analogue uptake in *S. cerevisiae* MaDH4 cells heterologously expressing *VvPLT1*.

Figure S10. *VvPLT1* gene expression analysis in mature leaves by real-time qPCR.

Figure S11. Quantification of sugars in full mature grape berries by HPLC in different irrigation treatments.

Figure S12. Aldose reductase (*VvA6PR*) gene expression analysis in mature leaves by real-time qPCR.

Table S1. Amino acid sequence identity of other putative VvPLTs.

Table S2. Abiotic stress-related *cis*-acting elements identified in the *VvPLT1* promoter sequence via PLACE.

Table S3. Abiotic stress-related *cis*-acting elements identified in the *VvMTD1* promoter sequence via PLACE.

Table S4. Sequences of the primers used in this study.

Acknowledgements

This work is supported by European Union Funds (FEDER/COMPETE-Operational Competitiveness Programme—INNOVINE—ref. 311775, and Enoexcel—Norte—07-0124-FEDER-000032), by Portuguese national funds (FCT-Portuguese Foundation for Science and Technology) under the project FCOMP-01-0124-FEDER-022692, the research projects PTDC/AGR-AAM/099154/2008 and PTDC/AGR-ALI/100636/2008, and the Will W. Lester Endowment of the University of California. AC was supported by an FCT PhD grant no. SFRH/BD/47699/2008. This work also benefited from the networking activities within the European-funded COST ACTION FA1106 ‘QualityFruit’. We thank Carlos Conde from the Instituto de Biologia Molecular e Celular (IBMC) for useful help and advice on confocal microscopy and imaging. We also thank Remi Lemoine from the Laboratoire de Physiologie et Biochimie Végétales, Centre National de la Recherche Scientifique UMR for kindly providing the MaDH4 yeast strain used in the heterologous expression studies.

References

- Abebe T, Guenzi AC, Martin B, Cushman JC.** 2003. Tolerance of mannitol-accumulating transgenic wheat to water stress and salinity. *Plant Physiology* **131**, 1748–1755.
- Afoufa-Bastien D, Medici A, Jeauffre J, Coutos-Thévenot P, Lemoine R, Atanassova R, Laloi M.** 2010. The *Vitis vinifera* sugar transporter gene family: phylogenetic overview and macroarray expression profiling. *BMC Plant Biology* **10**, 245.
- Ahuja I, de Vos RC, Bones AM, Hall RD.** 2010. Plant molecular stress responses face climate change. *Trends in Plant Science* **15**, 664–74.
- Bernsel A, Viklund H, Hennerdal A, Elofsson A.** 2009. TOPCONS: consensus prediction of membrane protein topology. *Nucleic Acids Research* **37**, W465–W468.
- Bieleski RL.** 1982. Sugar alcohols. In: Loewus A, Tanner W, eds. *Encyclopedia of plant physiology, New Series, vol. 13, part A. Plant carbohydrates*. Berlin: Springer, 158–192.
- Blom N, Gammeltoft S, Brunak S.** 1999. Sequence and structure-based prediction of eukaryotic protein phosphorylation sites. *Journal of Molecular Biology* **294**, 1351–1362.
- Blum A.** 2009. Effective use of water (EUW) and not water-use efficiency (WUE) is the target of crop yield improvement under drought stress. *Field Crop Research* **112**, 119–123.
- Bradford M.** 1976. A rapid and sensitive method for the quantitation of microgram quantities of protein utilizing the principle of protein–dye binding. *Analytical Biochemistry* **72**, 248–254.
- Calderón AA, Zapata JM, Barceló AR.** 1994. Differential expression of a cell wall-localized peroxidase isoenzyme capable of oxidizing 4-hydroxystilbenes during the cell culture of grapevine (*Vitis vinifera* cv. Airen and Monastrell). *Plant Cell, Tissue and Organ Culture* **37**, 121–127.
- Castellarin SD, Matthews MA, Di Gaspero G, Gambetta GA.** 2007. Water deficits accelerate ripening and induce changes in gene expression regulating flavonoid biosynthesis in grape berries. *Planta* **227**, 101–112.
- Chapman DM, Roby G, Ebeler SE, Guinard J-X, Matthews MA.** 2005. Sensory attributes of Cabernet Sauvignon wines made from vines with different water status. *Australian Journal of Grape and Wine Research* **11**, 329–347.
- Chaves MM, Santos TP, Souza CR, *et al.*** 2007. Deficit irrigation in grapevine improves water-use efficiency while controlling vigour and production quality. *Annals of Applied Biology* **150**, 237–252.
- Chaves MM, Zarrouk O, Francisco R, Costa JM, Santos T, Regalado AP, Rodrigues ML, Lopes CM.** 2010. Grapevine under deficit irrigation: hints from physiological and molecular data. *Annals of Botany* **105**, 661–676.
- Cimato A, Castelli S, Tattini M, Traversi ML.** 2010. An ecophysiological analysis of salinity tolerance in olive. *Environmental and Experimental Botany* **68**, 214–221.
- Conde C, Agasse A, Glissant D, Tavares RM, Gerós H, Delrot S.** 2006. Pathways of glucose regulation of monosaccharide transport in grape cells. *Plant Physiology* **141**, 1563–1577.

- Conde A, Chaves MM, Gerós H.** 2011a. Membrane transport, sensing and signaling in plant adaptation to environmental stress. *Plant and Cell Physiology* **52**, 1583–1602.
- Conde C, Delrot S, Gerós H.** 2008. Physiological, biochemical and molecular changes occurring during olive development and ripening. *Journal of Plant Physiology* **165**, 1545–1562.
- Conde A, Silva P, Agasse A, Conde C, Gerós H.** 2011b. Mannitol transport and mannitol dehydrogenase activities are coordinated in *Olea europaea* under salt and osmotic stresses. *Plant and Cell Physiology* **52**, 1766–1775.
- Conde C, Silva P, Agasse A, Lemoine R, Delrot S, Tavares R, Gerós H.** 2007a. Utilization and transport of mannitol in *Olea europaea* and implications for salt stress tolerance. *Plant and Cell Physiology* **48**, 42–53.
- Conde C, Silva P, Fontes N, Dias ACP, Tavares RM, Sousa MJ, Gerós H.** 2007b. Biochemical changes throughout grape berry development and fruit and wine quality. *Food* **1**, 1–22.
- Costa JM, Ortuño MF, Chaves MM.** 2007. Deficit irrigation as strategy to save water: physiology and potential application to horticulture. *Journal of Integrative Plant Biology* **49**, 1421–1434.
- Cramer GR, Ergul A, Grimplet J, et al.** 2007. Water and salinity stress in grapevines: early and late changes in transcript and metabolite profiles. *Functional and Integrative Genomics* **7**, 111–134.
- Decendit A, Ramawat KG, Waffo P, Deffieux G, Badoc A, Mérillon JM.** 1996. Anthocyanins, catechins, condensed tannins and piceid production in *Vitis vinifera* cell bioreactor cultures. *Biotechnology Letters* **18**, 659–662.
- Deluc LG, Grimplet J, Wheatley MD, Tillett RL, Quilici DR, Osborne C, Schooley DA, Schlauch KA, Cushman JC, Cramer GR.** 2007. Transcriptomic and metabolite analyses of Cabernet Sauvignon grape berry development. *BMC Genomics* **8**, 429.
- Deluc L, Quilici D, Decendit A, Grimplet J, Wheatley M, Schlauch K, Cramer G.** 2009. Water deficit alters differentially metabolic pathways affecting important flavor and quality traits in grape berries of Cabernet Sauvignon and Chardonnay. *BMC Genomics* **10**, 212.
- Donahue JL, Alford SR, Torabinejad J, et al.** 2010. The Arabidopsis *Myo*-inositol 1-phosphate synthase1 gene is required for *Myo*-inositol synthesis and suppression of cell death. *The Plant Cell* **22**, 888–903.
- Dry P, Loveys BR.** 1998. Factors influencing grapevine vigour and the potential for control with partial rootzone drying. *Australian Journal of Grape and Wine Research* **4**, 140–148.
- Escobar-Gutiérrez AJ, Zipperlin B, Carbonne F, Moing A, Gaudillère J-P.** 1998. Photosynthesis, carbon partitioning and metabolite content during drought stress in peach seedlings. *Australian Journal of Plant Physiology* **25**, 197–205.
- Eyégghé-Bickong HA., Alexandersson EO, Gouws LM, Young PR, Vivier MA.** 2012. Optimisation of an HPLC method for the simultaneous quantification of the major sugars and organic acids in grapevine berries. *Journal of Chromatography B* **885**, 43–49.
- FAO. 1998. Crop evapotranspiration. Allen RG, Pereira LS, Raes D, Smith M, eds. *Irrigation and drainage*, Paper No. 56. Rome: FAO.
- Fiehn O, Wohlgemuth G, Scholz MR.** 2005. Setup and annotation of metabolomic experiments by integrating biological and mass spectrometric metadata. *Data Integration in Life Sciences Proceedings* **3615**, 224–239.
- Fiehn O, Wohlgemuth G, Scholz MR, Kind T, Lee DY, Lu Y, Moon S, Nikolau B.** 2008. Quality control for plant metabolomics: reporting MSI-compliant studies. *The Plant Journal* **53**, 691–704.
- Flexas J, Bota J, Escalona JM, Sampol B, Medrano H.** 2002. Effects of drought on photosynthesis in grapevines under field conditions: an evaluation of stomatal and mesophyll limitations. *Functional Plant Biology* **29**, 461–471.
- Flexas J, Escalona JM, Medrano H.** 1998. Down-regulation of photosynthesis by drought underfield conditions in grapevine leaves. *Australian Journal of Plant Physiology* **25**, 893–900.
- Gao M, Tao R, Miura K, Dandekar AM, Sugiura A.** 2001. Transformation of Japanese persimmon (*Diospyros kaki Thunb.*) with apple cDNA encoding NADP-dependent sorbitol-6-phosphate dehydrogenase. *Plant Science* **160**, 837–845.
- Gao Z, Maurousset L, Lemoine R, Yoo SD, Van Nocker S, Loescher WH.** 2003. Cloning, expression, and characterization of sorbitol transporters from developing sour cherry fruit and leaf sink tissues. *Plant Physiology* **131**, 1566–1575.
- Gietz RD, Woods RA.** 2002. Transformation of yeast by the Liac/SS carrier DNA/PEG method. *Methods in Enzymology* **350**, 87–96.
- Grimplet J, Deluc LG, Cramer GR, Cushman JC.** 2007. Integrating functional genomics with abiotic stress responses in wine grape – *Vitis vinifera*. In: Jenks MA, Hasegawa PM, Jain SM, eds. *Advances in molecular breeding towards salinity and drought tolerance*. Dordrecht: Springer, 643–668.
- Hannah L, Roehrdanz PR, Ikegami M, Shepard AV, Shaw MR, Tabor G., Hijmans RJ.** 2013. Climate change, wine, and conservation. *Proceedings of the National Academy of Sciences, USA* **110**, 6907–6912.
- Higo K, Ugawa Y, Iwamoto M, Korenaga T.** 1999. Plant cis-acting regulatory DNA elements (PLACE) database. *Nucleic Acids Research* **27**, 297–300.
- Hu L, Lu H, Liu Q, Chen X, Jiang X.** 2005. Over-expression of *mtlD* gene in transgenic *Populus tomentosa* improves salt tolerance through accumulation of mannitol. *Tree Physiology* **25**, 1273–1281.
- Ishitani M, Majumder AL, Bornhouser A, Michalowski CB, Jensen RG, Bohnert HJ.** 1996. Coordinate transcriptional induction of *myo*-inositol metabolism during environmental stress. *The Plant Journal* **9**, 537–548.
- Jaillon O, Aury JM, Noel B, et al.** 2007. The grapevine genome sequence suggests ancestral hexaploidization in major angiosperm phyla. *Nature* **449**, 463–467.
- Jennings DB, Daub ME, Pharr DM, Williamson JD.** 2002. Constitutive expression of a celery mannitol dehydrogenase in tobacco enhances resistance to the mannitol-secreting fungal pathogen *Alternaria alternata*. *The Plant Journal* **32**, 41–49.
- Jennings DB, Ehrenschaft M, Pharr DM, Williamson JD.** 1998. Roles for mannitol and mannitol dehydrogenase in active oxygen-mediated plant defense. *Proceedings of the National Academy of Sciences, USA* **95**, 15129–15133.
- Juchaux-Cachau M, Landouar-Arsivaud L, Pichaut JP, Campion C, Porcheron B, Jeauffre J,... Lemoine R.** 2007. Characterization of AgMaT2, a plasma membrane mannitol transporter from celery, expressed in phloem cells, including phloem parenchyma cells. *Plant Physiology* **145**, 62–74.
- Kanehisa M, Goto S.** 2000. KEGG: Kyoto Encyclopedia of Genes and Genomes. *Nucleic Acids Research* **28**, 27–30.
- Karakas B, Ozias-Akins P, Stushnoff C, Sufferheld M, Rieger M.** 1997. Salinity and drought tolerance of mannitol-accumulating transgenic tobacco. *Plant, Cell and Environment* **20**, 609–616.
- Klepek YS, Geiger D, Stadler R, Klebl F, Landouar-Arsivaud L, Lemoine R, Hedrich R, Sauer N.** 2005. Arabidopsis POLYOL TRANSPORTER5, a new member of the monosaccharide transporter-like superfamily, mediates H⁺-symport of numerous substrates, including *myo*-inositol, glycerol, and ribose. *The Plant Cell* **17**, 204–218.
- Klepek YS, Volke M, Konrad KR, et al.** 2010. Arabidopsis thaliana POLYOL/MONOSACCHARIDE TRANSPORTERS 1 and 2: fructose and xylytol/H⁺ symporters in pollen and young xylem cells. *Journal of Experimental Botany* **61**, 537–550.
- Krasensky J, Jonak C.** 2012. Drought, salt, and temperature stress-induced metabolic rearrangements and regulatory networks. *Journal of Experimental Botany* **63**, 1593–1608.
- Lewis DH.** 1984. Physiology and metabolism of alditols. In: Lewis DH, ed. *Storage carbohydrates in vascular plants*. Cambridge: Cambridge University Press, 157–179.
- Loescher WH, Everard JD.** 1996. Sugar alcohol metabolism in sinks and sources. In: Zamski E, Schaffe AA, eds. *Photoassimilate distribution in plants and crops*. New York: Marcel Dekker, 185–207.
- Lorenz DH, Eichhorn KW, Bleiholder H, Klose R, Meier U, Weber E.** 1994. Phänologische Entwicklungsstadien der Weinrebe (*Vitis vinifera* L. ssp. vinifera). *Viticultural and Enological Sciences* **49**, 66–70.
- Maroco JP, Rodrigues ML, Lopes C, Chaves MM.** 2002. Limitations to leaf photosynthesis in field-grown grapevine under drought—metabolic and modelling approaches. *Functional Plant Biology* **29**, 451–459.
- Marsilio V, Campestre C, Lanza B, De Angelis M.** 2001. Sugar and polyol compositions of some European olive fruit varieties (*Olea europaea* L.) suitable for table olive purposes. *Food Chemistry* **72**, 485–490.

- Matthews MA, Anderson MM.** 1988. Fruit ripening in *Vitis vinifera* L. responses to seasonal water deficits. *American Journal of Enology and Viticulture* **39**, 313–320.
- Matthews MA, Anderson MM.** 1989. Reproductive development in grape (*Vitis vinifera* L.): responses to seasonal water deficits. *American Journal of Enology and Viticulture* **40**, 52–60.
- Matthews MA, Ishii R, Anderson MM, O'Mahony M.** 1990. Dependence of wine sensory attributes on vine water status. *Journal of the Science of Food and Agriculture* **51**, 321–335.
- Melgar JC, Guidi L, Remorini D, et al.** 2009. Antioxidant defenses and oxidative damage in salt-treated olive plants under contrasting sunlight irradiance. *Tree Physiology* **29**, 1187–1198.
- Meng PH, Raynaud C, Tcherkez G, Blanchet S, Massoud K, Domenichini S, Bergounioux C.** 2009. Crosstalks between myo-inositol metabolism, programmed cell death and basal immunity in Arabidopsis. *PLoS One* **4**, e7364.
- Merchant A, Richter AA.** 2011. Polyols as biomarkers and bioindicators for 21st century plant breeding. *Functional Plant Biology* **38**, 934–940.
- Moing A, Carbonne F, Zipperlin B, Svanella L, Gaudillère JP.** 1997. Phloem loading in peach: symplastic or apoplastic? *Physiologia Plantarum* **101**, 489–496.
- Murashige T, Skoog F.** 1962. A revised medium for rapid growth and bioassays with tobacco tissue cultures. *Physiologia Plantarum* **15**, 473–497.
- Nadwodnik J, Lohaus G.** 2008. Subcellular concentrations of sugar alcohols and sugars in relation to phloem translocation in *Plantago major*, *Plantago maritima*, *Prunus persica*, and *Apium graveolens*. *Planta* **227**, 1079–1089.
- Negm FB, Loescher WH.** 1981. Characterization and partial purification of aldose-6-phosphate reductase (alditol-6-phosphate:NADP 1-oxidoreductase) from apple leaves. *Plant Physiology* **67**, 139–142.
- Nelson DE, Rammesmayr G, Bohnert HJ.** 1998. Regulation of cell-specific inositol metabolism and transport in plant salinity tolerance. *The Plant Cell* **10**, 753–764.
- Nishizawa A, Yabuta Y, Shigeoka S.** 2008. Galactinol and raffinose constitute a novel function to protect plants from oxidative damage. *Plant Physiology* **147**, 1251–1263.
- Noiraud N, Maurousset L, Lemoine R.** 2001a. Identification of a mannitol transporter, AgMaT1, in celery phloem. *The Plant Cell* **13**, 695–705.
- Noiraud N, Maurousset L, Lemoine R.** 2001b. Transport of polyols in higher plants. *Plant Physiology and Biochemistry* **39**, 717–728.
- Ojeda H, Andary C, Kraeva E, Carboneau A, Deloire A.** 2002. Influence of pre- and postveraison water deficit on synthesis and concentration of skin phenolic compounds during berry growth of *Vitis vinifera* cv. Shiraz. *American Journal of Enology and Viticulture* **53**, 261–267.
- Pfaffl MW.** 2001. A new mathematical model for relative quantification in real-time RT-PCR. *Nucleic Acids Research* **29**, e45.
- Pillet J, Egert A, Pieri P, Lecourieux F, Kappel C, Charon J, Lecourieux D.** 2012. VvGOLS1 and VvHsfA2 are involved in the heat stress responses in grapevine berries. *Plant and Cell Physiology* **53**, 1776–1792.
- Pommerrenig B, Papini-Terzi FS, Sauer N.** 2007. Differential regulation of sorbitol and sucrose loading into the phloem of *Plantago major* in response to salt stress. *Plant Physiology* **144**, 1029–1038.
- Ramsperger-Gleixner M, Geiger D, Hedrich R, Sauer N.** 2004. Differential expression of sucrose transporter and polyol transporter genes during maturation of common plantain companion cells. *Plant Physiology* **134**, 147–160.
- Reid, KE, Olsson N, Schlosser J, Peng F, Lund ST.** 2006. An optimized grapevine RNA isolation procedure and statistical determination of reference genes for real-time RT-PCR during berry development. *BMC Plant Biology* **6**, 27.
- Reinders A, Panshyshyn JA, Ward JM.** 2005. Analysis transport activity of Arabidopsis sugar alcohol permease homolog AtPLT5. *Journal of Biological Chemistry* **280**, 1594–1602.
- Remorini D, Melgar JC, Guidi L, et al.** 2009. Interaction of root zone salinity and solar irradiance on the physiology and biochemistry of *Olea europaea*. *Environmental and Experimental Botany* **65**, 210–219.
- Roby G, Harbertson JF, Adams DA, Matthews MA.** 2004. Berry size and vine water deficits as factors in winegrape composition: anthocyanins and tannins. *Australian Journal of Grape and Wine Research* **10**, 100–107.
- Roubelakis-Angelakis KA, Kliewer WM.** 1979. The composition of bleeding sap from Thompson Seedless grapevines as affected by nitrogen fertilization. *American Journal of Enology and Viticulture* **30**, 14–18.
- Saidi Y, Finka A, Goloubinoff P.** 2011. Heat perception and signalling in plants: a tortuous path to thermotolerance. *New Phytologist* **190**, 556–565.
- Shen B, Hohmann S, Jensen RG, Bohnert HJ.** 1999. Roles of sugar alcohols in osmotic stress adaptation. Replacement of glycerol and mannitol and sorbitol in yeast. *Plant Physiology* **121**, 45–52.
- Shen B, Jensen RG, Bohnert HJ.** 1997a. Increased resistance to oxidative stress in transgenic plants by targeting mannitol biosynthesis to chloroplasts. *Plant Physiology* **113**, 1177–1183.
- Shen B, Jensen RG, Bohnert HJ.** 1997b. Mannitol protects against oxidation by hydroxyl radicals. *Plant Physiology* **115**, 527–532.
- Sheveleva E, Chmara W, Bohnert HJ, Jensen RG.** 1997. Increased salt and drought tolerance by D-ononitol production in transgenic *Nicotiana tabacum*. *Plant Physiology* **115**, 1211–1219.
- Souza CR, Maroco J, Santos T, et al.** 2005. Impact of deficit irrigation on water use efficiency and carbon isotope composition (^{13}C) of fieldgrown grapevines under Mediterranean climate. *Journal of Experimental Botany* **56**, 2163–2172.
- Stoop JMH, Pharr DM.** 1993. Effect of different carbon sources on relative growth rate, internal carbohydrates, and mannitol 1-oxidoreductase activity in celery suspension cultures. *Plant Physiology* **103**, 1001–1008.
- Stoop JMH, Williamson JD, Pharr DM.** 1996. Mannitol metabolism in plants: a method for coping with stress. *Trends in Plant Science* **5**, 139–144.
- Taji T, Ohsumi C, Iuchi S, Seki M, Kasuga M, Kobayashi M, Yamaguchi-Shinozaki K, Shinozaki K.** 2002. Important roles of drought- and cold inducible genes for galactinol synthase in stress tolerance in *Arabidopsis thaliana*. *The Plant Journal* **29**, 417–426.
- Tarczynski MC, Jensen RG, Bohnert HJ.** 1993. Stress protection of transgenic tobacco by production of the osmolyte mannitol. *Science* **259**, 508–510.
- Tari I, Kiss G, Deer AK, Csiszár J, Erdei L, Gallé Á, Simon LM.** 2010. Salicylic acid increased aldose reductase activity and sorbitol accumulation in tomato plants under salt stress. *Biologia Plantarum* **54**, 677–683.
- Tattersall EA, Grimplet J, Deluc L, et al.** 2007. Transcript abundance profiles reveal larger and more complex responses of grapevine to chilling compared to osmotic and salinity stress. *Functional and Integrative Genomics* **7**, 317–333.
- Thomas JC, Bohnert HJ.** 1993. Salt stress perception and plant growth regulators in the halophyte *Mesembryanthemum crystallinum*. *Plant Physiology* **103**, 1299–1304.
- Thomas JC, Sepahi M, Arendall B, Bohnert HJ.** 1995. Enhancement of seed germination in high salinity by engineering mannitol expression in *Arabidopsis thaliana*. *Plant, Cell and Environment* **18**, 801–806.
- Vincent D, Ergul A, Bohlman MC, et al.** 2007. Proteomic analysis reveals differences between *Vitis vinifera* L. cv. Chardonnay and cv. Cabernet Sauvignon and their responses to water deficit and salinity. *Journal of Experimental Botany* **58**, 1873–1892.
- Voegele RT, Hahn M, Lohaus G, Link T, Heiser I, Mendgen K.** 2004. Possible roles for mannitol and mannitol dehydrogenase in the biotrophic plant pathogen *Uromyces fabae*. *Plant Physiology* **137**, 190–198.
- Voinnet O, Rivas S, Mestre P, Baulcombe D.** 2003. An enhanced transient expression system in plants based on suppression of gene silencing by the p19 protein of tomato bushy stunt virus. *The Plant Journal* **33**, 949–956.
- Walbot V.** 2011. How plants cope with temperature stress. *BMC Biology* **9**, 79.
- Watari J, Kobae Y, Yamaki S, Yamada K, Toyofuku K, Tabuchi T, Shiratake K.** 2004. Identification of sorbitol transporters expressed in the phloem of apple source leaves. *Plant and Cell Physiology* **45**, 1032–1041.
- Williamson JD, Stoop JMH, Massel MO, Conkling MA, Pharr DM.** 1995. Sequence analysis of a mannitol dehydrogenase cDNA from plants reveals a function for the pathogenesis-related protein EL13. *Proceedings of the National Academy of Sciences, USA* **92**, 7148–7152.
- Zimmermann MH, Ziegler H.** 1975. List of sugars and sugar alcohols in sieve-tube exudates. In: Zimmermann MH, Milburn JA, eds. *Encyclopedia of plant physiology, vol. 1: transport in plants*. Berlin: Springer, 479–503.